4. Internationales Kolloquium
Werkstoffwissenschaften und Bauinstandsetzen
Technische Akademie Esslingen, 17.- 19. Dez. 1996

Repassivating Effects induced by Cathodic Protection of Rebars in Concrete

W. Schwarz, A. Gerdes, F.H. Wittmann, F. Pruckner* und G. E. Nauer*
Institut für Baustoffe, ETH-Zürich, CH-8093 Zürich
*Inst. f. physikalische Chemie, Universität Wien, A-1090 Wien

Abstract
Prolonged application of cathodic protection (CP) to the reinforcement induces at least partial repassivation whose extent and stability depends on the charge consumed during CP and on the Cl^-/OH^- ratio near the rebar surface after CP. In specimens with a chloride content of 3% by weight of cement a current consumption of $> 3\times10^5$ Cb/m^2 is required for the repassivation to remain stable for at least 40 days. The repassivating effect is assumed to be due to the alkalisation of the rebar surface during CP and due the formation of a secondary protective layer, consisting mainly of magnetite, formed at Cl^-/OH^- ratios < 1.

Repassivierende Wirkung des kathodischen Korrosionsschutzes auf die Bewehrung in Beton

Zusammenfassung
Kathodischer Korrosionsschutz bewirkt eine zumindest teilweise Repassivierung des Bewehrungsstahls. Ausmass und Dauerhaftigkeit der Repassivierung hängen von der während des kathodischen Schutzes verbrauchten elektrischen Ladung und von dem Cl^-/OH^- - Verhältnis an der Stahloberfläche nach dem Ausschalten des Schutzstromes ab. In Betonproben mit einem Chloridgehalt von 3% bezogen auf das Zementgewicht ist ein Ladungsverbrauch von $> 10^5$ Cb/m^2 erforderlich, um eine ausreichende Repassivierung über einen Zeitraum von mindestens 40 Tagen zu erreichen. Es wird angenommen, dass die Repassivierung auf der Alkalisierung der Stahloberfläche während des kathodischen Schutzes und auf einer bei Cl^-/OH^- - Verhältnissen < 1 gebildeten sekundären Schutzschicht (Magnetit) beruht.

1 Introduction

Corrosion of steel in concrete is one of the major problems with respect to the durability of reinforced concrete structures. The enormous amount of money required for repair measures results in a strong need to improve the durability of new structures as well as to guarantee the durability of existing structures after repair. Preventive protection or early intervention can be expected to be much more cost effective than waiting until damage occurs. However, if the concrete structure is already damaged, basically, the repair should interfere with the structural system as little as possible. This means that the removal of structurally sound concrete should be kept to the absolute minimum consistent with the chosen repair principle. The repair principles to restore corrosion protection need to be designed on the basis of the electrochemical corrosion processes within the surrounding concrete [1]. The electrochemical processes are governed principally by local potential differences on the rebars, oxygen concentration and humidity. If the local rebar potential drops below the "passive state" either by the reduction of the pH through carbonation of the alkaline-buffer calcium hydroxide or if the passive layer is destroyed by chloride ingress, local corrosion cells will be established and corrosion will start if sufficient humidity and oxygen are present.

There are four basic principles of corrosion protection: repassivation, limitation of the moisture content of concrete, coating of the reinforcement and cathodic protection [1]. Cathodic protection (CP) of steel in concrete is becoming a widely accepted and reliable method for fighting reinforcement corrosion, with a record going back two decades in the USA [1] and with more recent experiences in Europe e.g. in U.K [2], in Italy [3] and Switzerland [4]. CP has been applied recently to new structures: bridge decks in Italy[5-6] and a jetty deck in the UK [1]. This technique is referred to as "cathodic prevention" [1]. In general, CP is most suited to projects where conventional repair methods are not effective, which is usually associated with high chloride levels at the steel. An advantage is that removal of chloride contaminated but structurally sound concrete is unnecessary[1].

The main aim of CP is to shift the potential difference between the steel and the concrete pore solution towards more negative values, where the corrosion rate is decreased to an insignificant level, by applying electric current from an external source. This shift has to be maintained over the remaining lifetime of the structure [7]. Besides the potential shift of the reinforcement, CP has beneficial effects on the corrosion behaviour of reinforcement in concrete: elimination of corrosion cells [4], reduction of the intrinsic corrosion [8], removal of chloride ions by electromigration [8] and alkalisation of the pore solution near the rebar surface [9]. However, with regard to the alkalisation of the pore solution the presence of alkali-reactive aggregates [10] should be checked for. The influence of the acid produced at the anode on the concrete properties should also be considered [3,11].

Early results on the evaluation of CP on the corrosion behaviour of steel in chloride contaminated concrete suggested a reduced corrosion rate after the prolonged application of CP (1.2 years, av. current density 30 mA/m^2). After the CP system was off and disconnected for one month, the corrosion currents measured were about one

fourth of the corrosion currents before CP and the static half-cell potential of the rebars moved towards more noble values from an average potential of - 422 mV vs. CSE to about - 134 mV vs. CSE [12]. Similar results were obtained by Green et al. [13] though at significantly higher current densities during electrochemical extraction treatments. Significant repassivating effects were observed by linear polarisation resistance (LPR)- and electrochemical impedance spectroscopy (EIS)-measurements in chloride containing concrete specimens after the application of CP of only 1.5 month with current densities of about 2 - 50 mA/m^2 [14].

In the present work results on the passivating effect of CP of rebars in chloride contaminated concrete over a period of about 5 month are presented. The persistence, stability and extent of the repassivating effect of CP have been studied as a function of the charge consumed during CP and of the chloride content of the concrete slabs. The measurements and evaluations were carried out using LPR -, Tafel-, potential-measurements and EIS.

2 Background

The initial protection of the embedded steel is due to the formation of a self generating, adherent iron oxide layer of about 1 - 100 nm thickness [15-17], in the alkaline environment of the concrete matrix (pH 12.5 to 13.6 [18]). A wide range of compositions have been proposed for this passive layer. In the specific environment of concrete, the oxide layer consists of a Fe_3O_4 - γ -Fe_2O_3-spinel [15]. The results which have been reported by a number of authors suggest that the steel reinforcement tends to be surrounded by a thin layer of massive $Ca(OH)_2$-crystals [19-21], which imparts an additional physical protection to the steel [22]. The importance of this $Ca(OH)_2$-layer for the corrosion protection is disputed by Sagoe-Crentsil & Glasser [15] who propose a duplex layer model for the passivating layer in real structures, in which the steel is assumed to be in a semi-passive state and in which considerable interaction between the steel/passivating layer/cement occurs: The inner layer consists of the Fe_3O_4 - γ-Fe_2O_3-spinel phase containing sparsely distributed $Ca(OH)_2$ crystals, the outer reaction zone consists of poorly crystallised α-FeOOH and spinel and an increasing concentration of $Ca(OH)_2$ across the zone peaking at the outer layer/concrete boundary. The growth of the outer layer depends on the stability of the inner layer, which determines the extent of passivation and which is largely controlled by chloride ion concentration and the extent of carbonation of the concrete matrix. The ingress of CO_2, once the alkaline constituents of the concrete matrix are exhausted, leads to a rapid decrease of pH, which destabilises the passive layer (pH < 10) and stabilises α-FeOOH. If the chloride ion concentration at the steel surface exceeds a critical limit, then destabilisation of the passive layer occurs also in alkaline environments. The critical chloride contents for initiating corrosion are in the range between 0.48% and 2.02% by weight of cement [23]. The ENV 206 sets the maximum permissible total chloride content in reinforced concrete to 0.4 % and in prestressed concretes to 0.2% by weight of cement. The American Concrete Institute

[24] suggests for reinforced concrete an upper limit of 0.10% for the total soluble chloride and 0.06% for prestressed concrete. Chloride levels as low as 0.01 wt.% cement can initiate the process of depassivation [15]. However, it appears, that not the absolute chloride content but rather the ratio of Cl^-/OH^- in the pore solution determines the risk and the rate of corrosion [25-27]. Though several theories have been proposed to explain the role of chloride ions in the breakdown of passivity [16,28-31], the exact nature of the reaction is not yet fully understood. The type of corrosion products formed in the outer layer depend on the steel potential and on the pH [16,32].

Distinct from carbonation which induces uniform corrosion over a wide area of the steel surface [33] is the chloride ion induced corrosion localised ("pitting corrosion"). In order for corrosion to take place, corrosion cells have to be formed. A corrosion cell consists of an anode, where iron is oxidised to corrosion products, a cathode, where oxygen is reduced and an electrolyte (pore-solution) connecting anode and cathode. Carbonation induces the formation of microcells whereas chloride-induced corrosion leads to the formation of macrocells, with pits acting as anodes and the neighbouring sections of the passive rebar as cathodes (figure 1).

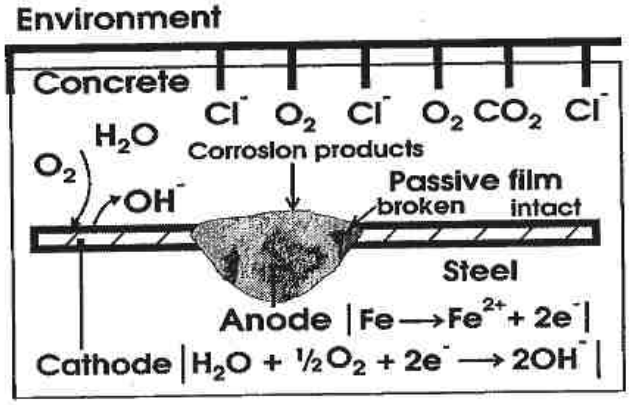

Fig. 1: Model for the corrosion of rebars within concrete [34].
Abb. 1:Schematische Darstellung einer Korrosionszelle [34)]

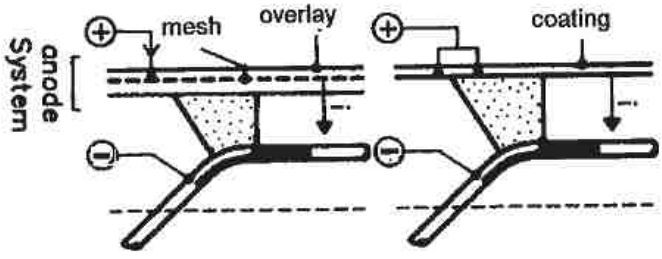

Fig. 2: Principle of the cathodic protection of reinforcement [1]
Abb. 2:Schema des kathodischen Korrosionschutz in Beton. [1]

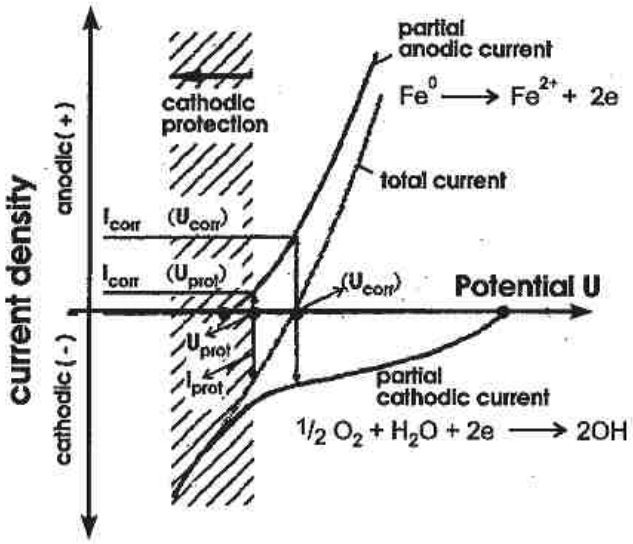

Fig. 3: Potential dependence of the anodic, cathodic partial and the total current densities for uniform corrosion. [37]

Abb. 3: Potentialabhängigkeit der anodischen und kathodischen Teilstrom- sowie der Gesamtstromdichten für den Fall einer gleichmässigen Korrosion [37]

The cathodic polarisation results in a reduction of the corrosive local anodic current at the expense of the corrosive anodic partial current and in an increase of the cathodic current (figure 3). Oxygen instead of being reduced by the corroding rebar is then principally reduced by the supplied CP current.

3 Materials and experimental procedures

3.1 Materials

Concrete prisms of 4.5 × 8 × 20 cm size were cast from concretes prepared with a water/cement ratio of 0.5 and 300 kg/m^3 cement and with different chloride contents (0%, 1%, 2%, 3% by weight of cement) added as NaCl. Dry sand of grain size 0/4 mm and 4/9 mm was used in a weight ratio of 1:1 as aggregate. Reinforcing steel bars with a diameter of 8 mm were axially positioned within the prisms giving a minimum of 2 cm concrete cover. Two graphite rods, serving as reference electrodes, were embedded in parallel to the steel bar into the fresh concrete prisms. The specimens were cured at 90% r.h. and ambient room temperature for 28 days, followed by three month at 80% r.h. and ambient room temperature. After demolding, the exposed part of the rebar and the surrounding concrete surface were coated with epoxy resin. As anode material for the cathodic protection, either a conductive carbon filled polymer coating or a titanium mesh (mesh size av. 45 mm) was used. The conductive polymer coating was applied on both sides of the prisms after demolding.

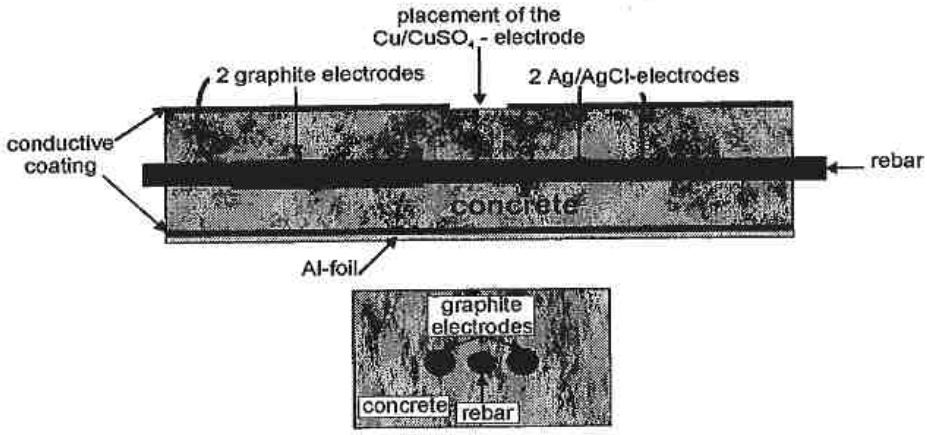

Fig. 4: Schematic presentation of the concrete prisms on which CP was applied and used for electrochemical measurements.

Abb. 4: Schematische Darstellung der für den kathodischen Schutz und für die elektrochemischen Messungen verwendeten Betonprismen.

Electrical contact to the polymer coating on one side consisted of a woven silver ribbon embedded in the coating and a metal foil was placed on the top surface of the coating on the other side to ensure an uniform current distribution (figure 4). The titanium mesh was embedded in the fresh concrete on one prism surface, electrical contact was made by copper wires. The following treatments were applied to the specimens:

After cathodic protection, the prisms were stored for approx. 4.5 months at ambient temperature at 80 - 90% r.h. Then the specimens were divided into two groups. One group was stored under water for 24 hours and the second group was exposed to three wet/dry cycles in a 3% NaCl solution. For the storage under water, the specimens were placed in a water tank, filled with water up to 50% of specimen height, after 4 h, water was added until the specimens were immersed completely 1 cm below the water level. After 24 h of storage under water, the specimens were stored at ambient atmosphere for 24 h, then dried at 50° C for three days and then equilibrated for two days at 80% r.h. at ambient room temperature. For the first wet/dry cycle the specimens were, after immersion for 24 h in a 3% NaCl solution, dried for 24 h at ambient atmosphere and then dried for 12h at 50° C. For the following two cycles the specimens were, after equilibration at room temperature for 4 h, immersed for 24 h in the 3% NaCl solution and subsequently dried for 12 h at 50° C. After completion of the wet/dry cycles, the specimens were dried for 3 days at 50°C and equilibrated at 80% r.h. for two days at room temperature.

3.2. Cathodic protection (CP)

For CP a constant voltage between the rebar and the anode has been applied to the specimens for about 4 months at 80 - 90% r.h. The voltage was 2V on one group of specimens and 1.6V on an group. The prisms with titanium mesh anodes were polarised with 2 V.

3.3. Electrochemical measurements

For the linear polarisation resistance- (LPR), electrochemical impedance spectroscopy- (EIS) and Tafel measurements, the conductive polymer covered with a metal foil was used as a counter electrode (figure 4). For the measurements on prisms with Ti-mesh anodes, the Ti-anode was used as counter electrode. The LPR, EIS and Tafel measurements were performed with graphite reference electrodes embedded in the prism and the potential measurements with a $Cu/CuSO_{4(sat)}$-reference electrode (CSE).

LPR measurements were carried out by applying cyclic voltage scans around the equilibrium potential of the rebars with an amplitude of ± 10 mV in 1.22 mV/16s steps. The measurements were carried out using an IBM compatible PC-AT-386/33 with a specially designed 12 bit A/D interface (Burr Brown ADC 80). A STV function generator (12 bit/ ± 2.5 V) connected via RS 232 was used via the software package CSTATIE [38]. The polarisation resistance (R_p) was determined according to the Stern´s relation. The LPR measurements are described elsewhere in detail [39]. I_{corr} calculated using a Butler-Volmer constant B of 0.025V, calculated from LPR- and Tafel- measurements are in agreement with published results [40].

For the Tafel measurements the same experimental set-up and software was used as for the LPR measurements. A scan of 100 mV in the anodic direction in 1.22 mV/16 s steps starting at the equilibrium potential of the rebar was applied. The anodic Tafel slope and I_{corr} was determined using the current values in the potential range between 60 and 100 mV.

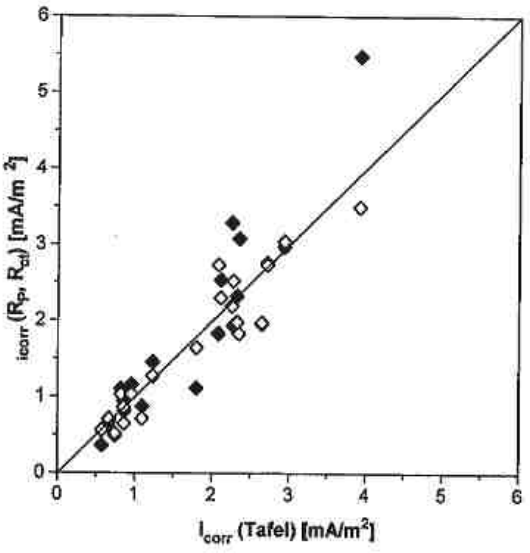

Fig. 5: Comparison of I_{corr} values calculated from LPR- (◊) and EIS- (♦) with I_{corr} values calculated from Tafel - measurements.

Abb. 5: Vergleich von aus LPR (◊)- und EIS (♦)- Messungen erhaltenen I_{corr}-Werten mit I_{corr} Werten aus Tafelmessungen.

Impedance measurements were performed using a FFT-based system consisting of a fast rising potentiostat (IMP 88, Jaissle, BRD), a dual channel FFT-analyser (TR 9404, Advantest, Japan) and a digital function generator (TR 98202, Advantest, Japan) controlled via GPIB by an IBM compatible PC-AT 486/25. Data analysis was done using Boukamps impedance software [14]. The FFT-analyser and the function generator were used in single sine sweep mode to avoid erroneous evaluation of non-linear response of the system. About 50 sine waves at a peak to peak amplitude of 20 mV in the frequency range from 25 mHz to 5.125 kHz were applied and the response registered in each run. I_{corr} was calculated from the obtained charge transfer resistance values R_{ct} using the same Butler-Volmer constant as for the LPR measurements [14]. I_{corr} values calculated from LPR-, EIS- and Tafel measurements showed good agreement (figure 5).

The concrete resistance was measured applying a 20 mV peak to peak amplitude/5000 Hz sine wave between the two opposite conductive coatings (figure 4). The determination of the chloride concentration in the pore solution of the concrete prisms was done using embedded Ag/AgCl - reference electrodes (figure 4) according to the method of Molina [41]. Before embedding, the electrodes were calibrated in artificial pore-solution (saturated $Ca(OH)_2$-solution) with different chloride contents.

4 Results and Discussion

Figure 6 shows the current flow between the anode and the rebar during CP of concrete prisms with different chloride contents and different anode materials at a constant CP-potential of 2 V over a time period of approximately 4 months. The protective current increases with increasing chloride content due to the decreasing concrete resistance R_Ω and decreasing transfer resistance R_{CT} at the rebar/pore solution interface [14].

At a given applied voltage and chloride content, the Ti-mesh anode delivers higher current densities than the conducting polymer anode. This might be due to a lower transfer resistance at the anode-concrete interface in comparison to the polymer anode-concrete interface.

Figure 7 a shows the corrosion current densities I_{corr}, calculated from Tafel-plots, before and after applying CP to rebars in concrete prisms with different chloride contents and different anode materials.

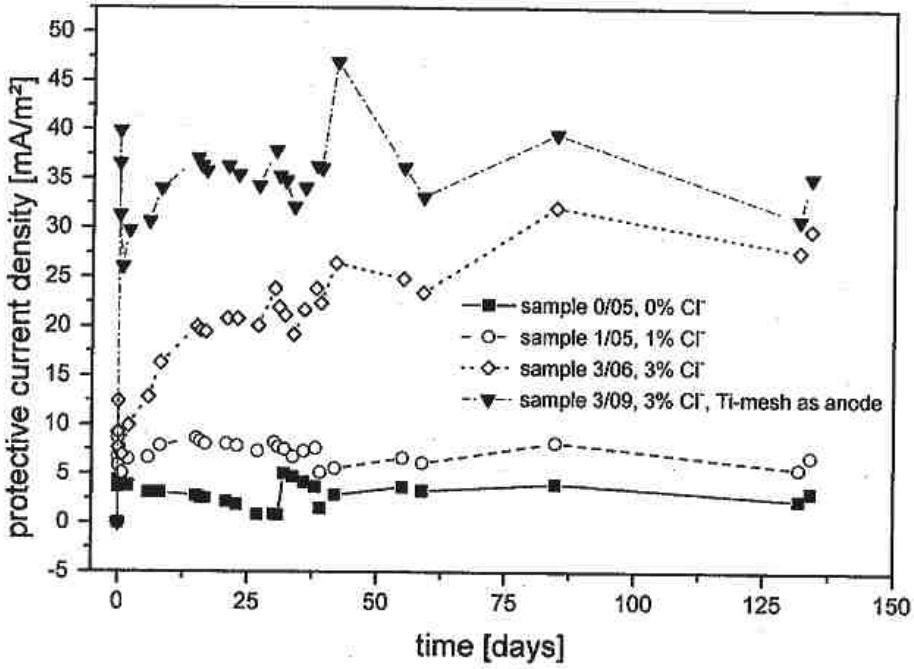

Fig. 6: Current densities during CP (protection voltage 2V) in concrete prisms with different chloride contents and different anode materials.

Abb. 6: Schutzstromdichten während der Anwendung des kathodischen Schutzes (Schutzspannung 2.0 V) auf Betonprismen mit unterschiedlichen Chloridgehalten und Anodenmaterialien.

I_{corr} measured before the application of CP increase significantly with the chloride content of the concrete prism. Andrade et al. [42] set the boundary between active and insignificant corrosion at 1 - 2 mA/m^2 (hatched area in figure 7 b). According to this criterion, the rebars in the specimens with a chloride content of 2% and 3% corrode actively whereas in specimens containing 1% chloride the I_{corr} values lie in the intermediate range between active and insignificant corrosion. After the application of CP for approximately 4 months, the I_{corr} values are significantly lower. The difference between I_{corr} values before and after CP increases with increasing chloride content of the specimen. In chloride-free reference samples, CP has no effect on the I_{corr} values. In the specimens with a chloride content of 3%, the rapid decrease of I_{corr} within the first few days after CP is attributed to the repassivation of the rebars. I_{corr} tends to decrease further over a time period of approximately 40 days after switching-off CP in all samples, except in the specimen with 1% chloride content in which I_{corr} remains nearly stable. Except for the specimens with a chloride content of 3% covered by the conductive polymer anode, all corrosion current values measured 40 days after switching-off CP are in the range of insignificant corrosion. After 140 days

storage after CP, the corrosion currents increase in all samples except in the chloride-free reference specimens. The specimens with 3% chloride (Ti-anode) and 1% chloride lie in the domain of insignificant corrosion, the specimen with 2% and 3% chloride (polymer anode) are situated in the intermediate range between insignificant and active corrosion. The corrosion currents 110 days after switching-off CP are significantly below the values before CP except for the specimens containing 1% chloride.

The corrosion potentials of the rebars show the same trends (figure 7 b). The corrosion potentials before the application of CP decrease towards negative values with increasing chloride content of the concrete prisms. Significant corrosion is observed in the specimens containing 2% and 3% chloride, according to the ASTM C 876-80 standard which sets the threshold value for 95% probability of corrosion at a potential of - 350 mV vs CSE. The corrosion potential of the specimens containing 1% chloride (- 322 mV vs. CSE) is in the intermediate range (- 200 to - 350 mV vs. CSE) in which corrosion is uncertain (hatched area in figure 7 b).

After application of CP, the corrosion potentials are shifted significantly towards positive values. In agreement with the I_{corr} values, repassivation is observed during the first few days after switching-off CP in the specimens containing 3% chloride. Up to 40 days after switching-off CP, the corrosion potentials tend to increase further with the exception of the specimen with a chloride content of 1%, in which E_{corr} approaches the E_{corr}-value before CP almost linearly with time over a time period of about 110 days. The specimens with 1% and 2% chloride remain in the potential domain of insignificant corrosion, the specimen with 3% chloride in the range of uncertain but near the edge to insignificant corrosion.

The corrosion potentials decrease significantly after 100 days akin to the corrosion current values. However, they remain significantly more positive than the corrosion potentials before CP. All corrosion potential values remain in the domain of uncertain corrosion as set by the ASTM C 876-80 standard. The positive shift of the corrosion potential of the chloride-free reference specimens might indicate the formation of a more passivating layer after CP. On the other hand, the corrosion current did not change after CP (figure 7 a). However, this might be due to the fact that the measured values are close to the detection limit of the equipment used.

Figure 8 shows the development of the corrosion potential after switching-off CP of the rebars in specimens containing 3% chloride.

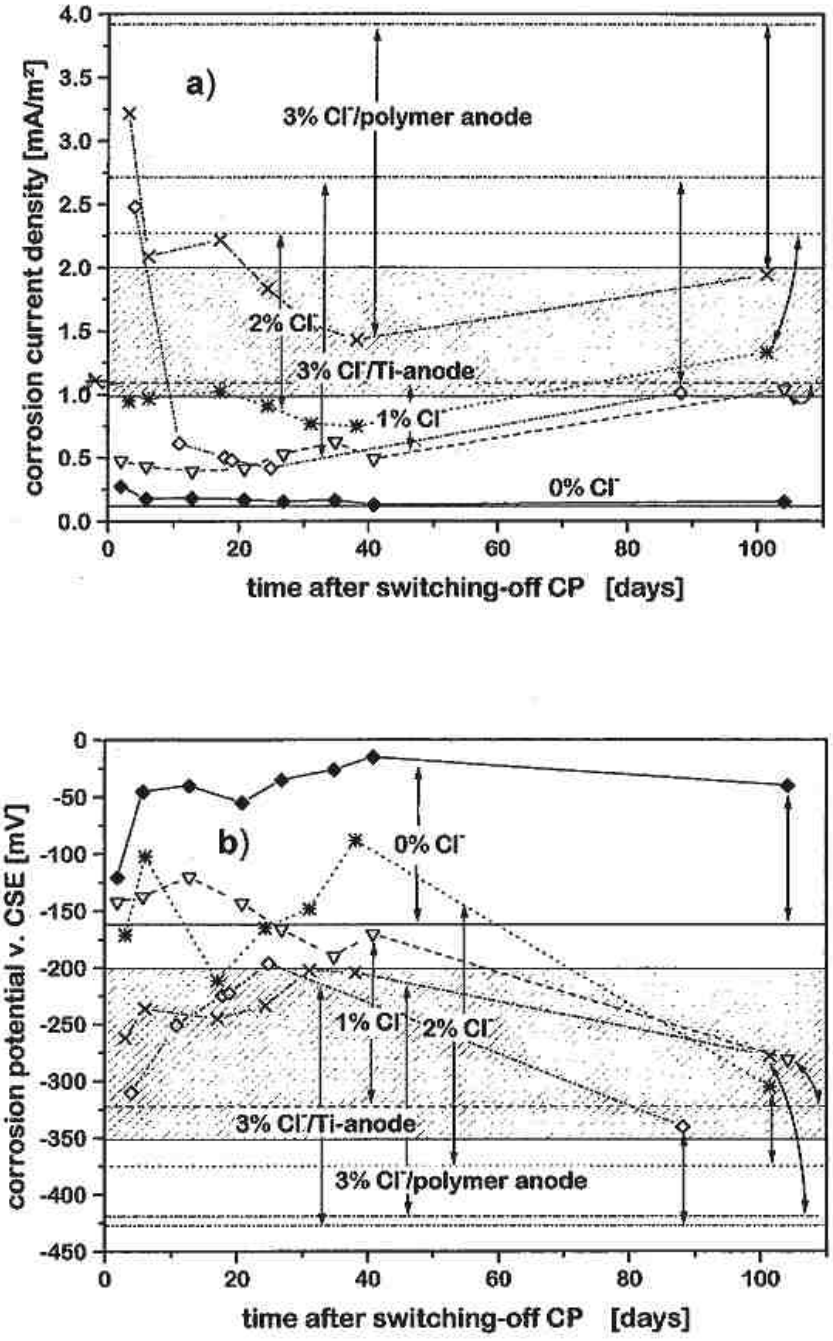

Fig. 7: Corrosion current densities (a) and Corrosion potentials (b) before (straight lines) and after cathodic protection (CP-voltage 2V) as function of the storage time (80% r.h.) for different chloride contents and anode materials.

Abb. 7: Korrosionstromdichten (a) und Korrosionspotentiale (b) vor (waagrechte Linien) und nach dem Abschalten des Schutzstromes (Schutzspannung 2V) als Funktion der Lagerungszeit (80% r.F.) für unterschiedliche Chloridgehalte und Anodenmaterialien.

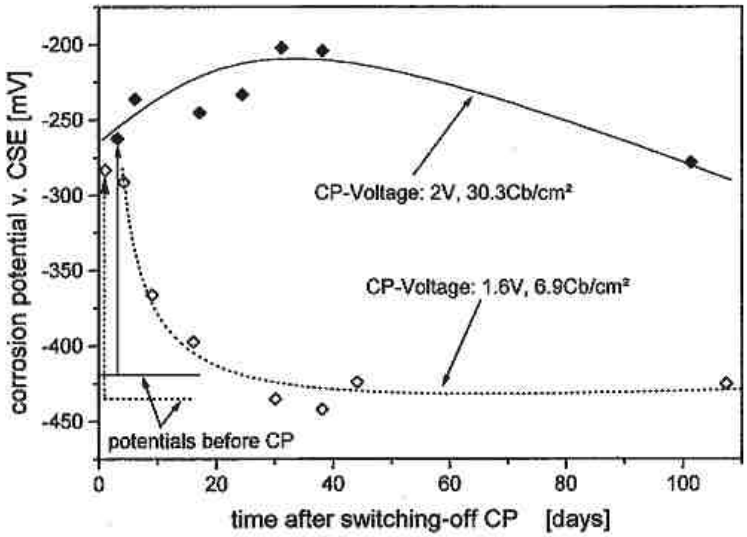

Fig. 8: Corrosion potentials at different applied CP-voltages as function of time after switching-off CP.

Abb. 8: Korrosionspotential in Abhängigkeit der Zeit nach Abschalten der Schutzspannung.

In both specimens, the rebar potentials are shifted by about 210 mV towards a potential value of about - 270 mV vs. CSE. The corrosion potentials of the rebar polarised at 2 V for 135 days increase by about 40 mV probably due to the repassivation of the rebar. The repassivation remains nearly stable for at least 40 days and decreases only slightly after 110 days. The corrosion potential of the rebar after switching-off CP decrease within 30 days to the corrosion potential before the application of CP.

For the evaluation of the stability of the repassivation after CP, the shifts of E_{corr} before and after CP (figure 9 a) and the ratio of $I_{corr.}^{after\ CP} / I_{corr.}^{before\ CP}$ (figure 9 b) were plotted against the time after switching-off CP.

Shortly after switching-off CP nearly the same shift of $E_{corr.}^{after\ CP} - E_{corr.}^{before\ CP}$ (120 - 180 mV) towards positive potential values, is observed (figure 9 a), except for one specimen (11.1×10^4 Cb/m^2). The results indicate, that the stability of the potential shift over time depends on the charge consumed during CP. The positive potential shifts of the specimens with high charge consumption (> 30×10^4 Cb/m^2) during CP tends to increase for at least 40 days after switching-off CP whereas the potential shifts of the specimens with low charge consumption (< 17×10^4 Cb/m^2), after a short increase, decrease over time towards the potential values measured before the application of CP. The initial short increase of the potential shift of these specimens appears also to correlate with the charge consumed during CP. The specimen which consumed 16.8×10^4 Cb/m^2 during CP shows an initial potential shift of about 150 mV towards positive values whereas the specimen which consumed 11.1×10^4 Cb/m^2

shows only a small potential shift and the specimen which consumed 6.9×10^4 Cb/m^2 shows nearly no initial shift at all.

The $I_{corr.}^{after\ CP} / I_{corr.}^{before\ CP}$ values show similar behaviour (figure 9 b). Shortly after switching of CP, the values are nearly of the same magnitude than before CP with the exception of the specimen which consumed 40.6×10^4 Cb/m^2 during CP. The $I_{corr.}^{after\ CP} / I_{corr.}^{before\ CP}$ values of the specimen which consumed > 30×10^4 Cb/m^2 during CP decrease at least for 40 days after switching-off CP whereas the $I_{corr.}^{after\ CP} / I_{corr.}^{before\ CP}$ values of the specimen which consumed < 17×10^4 Cb/m^2 tend to increase after switching-off CP. In agreement with the potential shifts (figure 9 b), the $I_{corr.}^{after\ CP} / I_{corr.}^{before\ CP}$ of the specimen with low charge consumption during CP decrease initially. The extent of this initial I_{corr} - decrease increases with the amount of charge consumed during CP. The specimen which consumed 16.8×10^4 Cb/m^2 during CP show the largest initial decrease of the I_{corr} values in comparison with the specimens with a charge consumption of 11.1×10^4 Cb/m^2 and 6.9×10^4 Cb/m^2, the latter one exhibits nearly no initial I_{corr} reduction at all.

The increase of the E_{corr} values and the reduction of the I_{corr} values after CP is attributed, as mentioned already above, to the repassivation of the rebars after switching-off CP. The $I_{corr.}^{after\ CP} / I_{corr.}^{before\ CP}$ values correlate in their tendencies with the $E_{corr.}^{after\ CP} - E_{corr.}^{before\ CP}$ values but not in their absolute values: The E_{corr} values of all specimen show significant potential shifts towards positive values shortly after switching-off CP in comparison with the Ecorr values before CP (figure 9 a) whereas the I_{corr} values of all specimen with the exception of the specimen which consumed 40.6×10^4 Cb/m^2 during CP, are of nearly the same magnitude than before CP. The specimen which consumed 40.6×10^4 Cb/m^2 during CP shows even higher I_{corr} values than before CP. This is attributed to the high sensitivity of I_{corr} towards the humidity in the specimens [43].

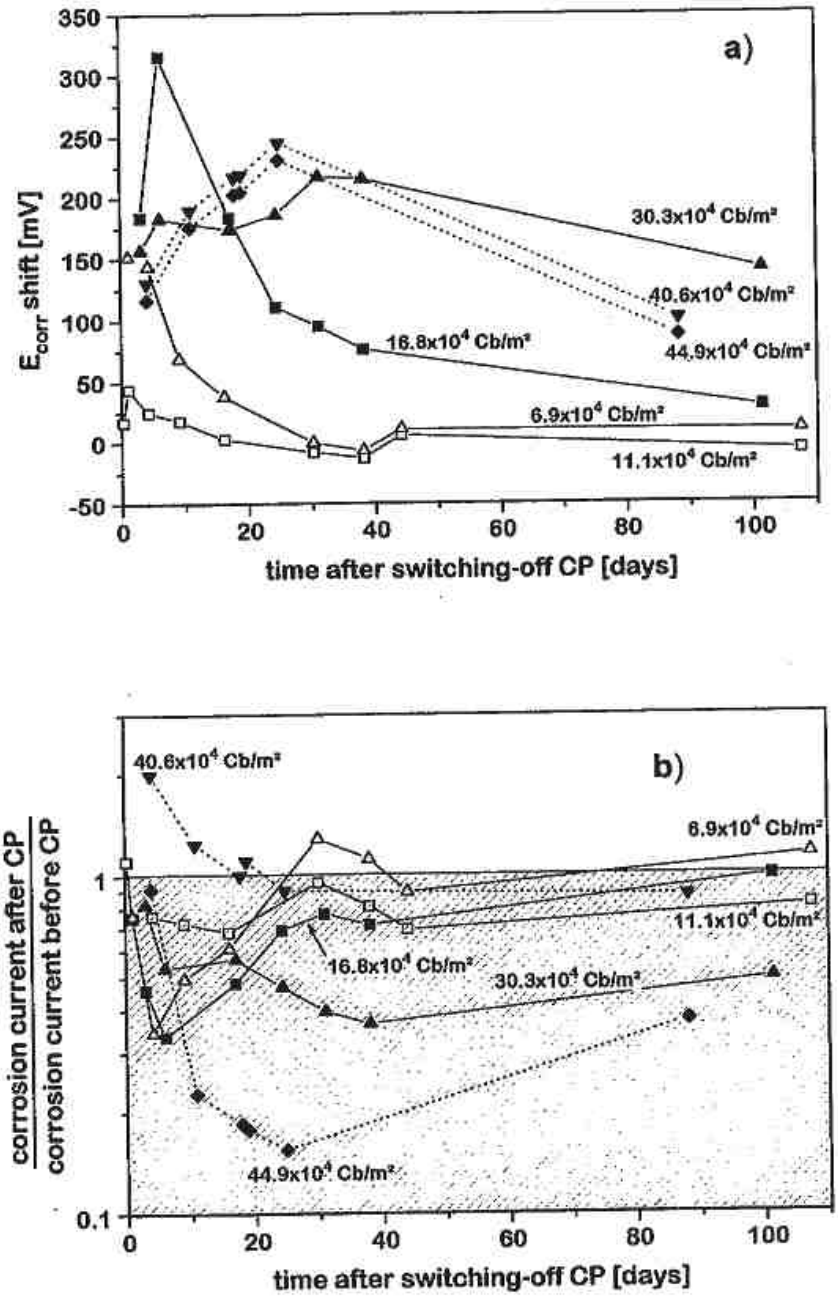

Fig. 9: $E_{corr.}^{after\ CP} - E_{corr.}^{before\ CP}$ (a) and $I_{corr.}^{after\ CP} / I_{corr.}^{before\ CP}$ (b) over time of rebars in concrete prisms (3% chloride) CP with 1.6 V (empty symbols) and 2 V (filled symbols) with conductive polymer anodes (solid lines) or titanium mesh anodes (dotted lines).

Abb. 9: $E_{corr.}^{nach\ KS} - E_{corr.}^{vor\ KS}$ *(a) und* $I_{corr.}^{nach\ KS} / I_{corr.}^{vor\ KS}$ *(b) von Bewehrungsstahl in Betonprismen (3% Chlorid), Schutzspannung 1.6 V (leere Symbole) und 2 V (gefüllte Symbole) mit leitenden Polymeranoden (ausgezogene Linien) oder Titannetzanoden (strichlierte Linien) in Abhängigkeit von der Zeit nach dem Abschalten des Schutzstromes.*

The stability and the relative values of corrosion potentials and corrosion currents after switching-off CP appear to correlate with the charge consumed during CP and not with the CP-voltage applied as shown in figures 10 and 11.

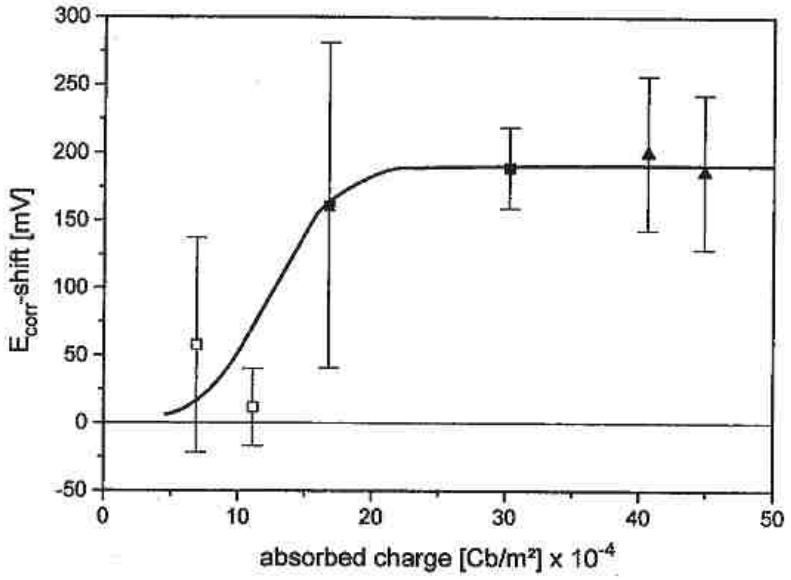

Fig. 10: $E_{corr.}^{after\ CP} - E_{corr.}^{before\ CP}$ in relation to the charge consumed during CP of rebars in concrete prisms (3% chloride), CP with 1.6 V (empty symbols) and 2 V (filled symbols) with conductive polymer anodes (v) or titanium mesh anodes (σ).

Abb. 10: $E_{corr.}^{nach\ KS} - E_{corr.}^{vor\ KS}$ *von Bewehrungsstahl in Betonprismen (3% Chlorid),Schutzspannung 1.6 V (leere Symbole) und 2 V (gefüllte Symbole) mit leitenden Polymeranoden*(v) *oder Titannetzanoden* (σ) *in Abhängigkeit von der Zeit.*

In figure 10, the values of $E_{corr.}^{after\ CP} - E_{corr.}^{before\ CP}$ measured between three and forty days after switching-off CP are plotted against the electric charge consumed during CP (vertical bars). The variation of the potential shift (E_{corr} - shift) of the first three specimens is mainly due to the decrease of E_{corr} after CP towards the E_{corr} before CP (E_{corr} - shift = 0) and not due to scatter. The variation of E_{corr} at higher consumed charges during CP (> $20'10^4$ Cb/m^2) is mainly due to the variation around a nearly stable level (figure 9). The symbols in figure 10 represent the mean values of the potential variations weighted for the time of measurement. As shown in figure 10, the mean values of the potential variations increase significantly up to a consumed charge during CP of about $20'10^4$ Cb/m^2 and then remain nearly independent of the absorbed charge.

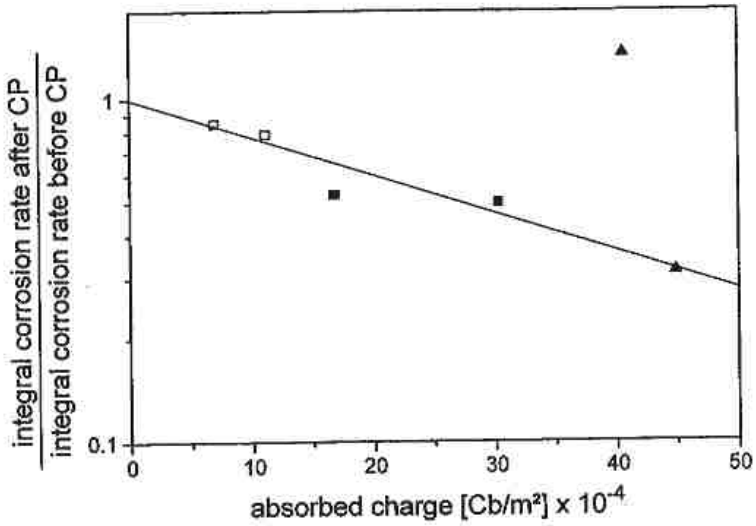

Fig. 11: $\overline{i_{corr}^{after\ CP}} / i_{corr}^{before\ CP}$ in relation to the charge consumed during CP of rebars in concrete prisms (3% chloride) CP with 1.6 V (empty symbols) and 2 V (filled symbols) with conductive polymer anodes (v) or titanium mesh anodes (σ).

Abb. 11: $\overline{i_{korr}^{nach\ KS}} / i_{korr}^{vor\ KS}$ *von Bewehrungsstahl in Betonprismen (3% Chlorid), Schutzspannung 1.6 V (leere Symbole) und 2 V (gefüllte Symbole) mit leitenden Polymeranoden*(v) *oder Titannetzanoden* (σ) *in Abhängigkeit umgesetzten Ladung.*

In figure 11, the logarithm of the mean corrosion current after switching-off CP ($\overline{i_{corr}^{after\ CP}} = \left(\int_{t_1\cong 3d}^{t_2\cong 40d} I_{corr}\, dt\right) / (t_1 - t_2)$) decreases linearly with the charge consumed during CP, except for the value determined in the specimen which consumed 40.6×10^4 Cb/m^2 (see figure 9). The exponential decrease of $\overline{i_{corr}^{after\ CP}} / i_{corr}^{before\ CP}$ is due to the exponential current/potential dependence.

From the correlation of E_{corr}-shift and of the mean corrosion currents $\overline{i_{corr}^{after\ CP}} / i_{corr}^{before\ CP}$ with the charge consumed during CP, it is concluded that the repassivation of rebars after switching-off CP is initiated by products formed by electrochemical reactions during CP. The repassivation of rebars in specimens with a chloride content of 3% which have consumed ≥ 30´10^4 Cb/m^2 during CP appear to be stable for a minimum of 40 days after switching-off CP. This might indicate that a minimum amount of products has to be formed during CP to allow a stable repassivation for at least 40 days.

The possible electrochemical reactions taking place during CP are determined by the half-cell potential of the rebar. In figure 12, the half-cell potentials of rebars

during CP of specimens (assuming a pH of 13.2 of the pore solution) with a chloride content varying between 0% and 3% and a CP - voltage of 1.6 and 2V with conductive polymer anodes or titanium mesh anodes are shown in relation to the standard-half-cell-potentials of possible electrochemical reactions as a function of the pH [44].

As figure 12 shows, the only feasible cathodic reaction which is able to maintain the cathodic polarisation current during CP is the reduction of oxygen:

$$0_2 + 4H_2O + 4e^- = 4OH^- \quad (1)$$

However, the half-cell potentials of rebars polarised with a CP-voltage of 2V using Ti-mesh anodes are close to the standard-half-cell potential of the reduction of solid iron(III)hydroxide ($Fe(OH)_{3(s)}$). Therefore, part of the cathodic polarisation current of specimens with Ti-mesh anodes might be due to the reduction of iron(III)hydroxides near the rebar surface. At the applied potentials during CP, the reduction of water to hydrogen as well as the reduction of iron(II)hydroxid to iron can be ruled out.

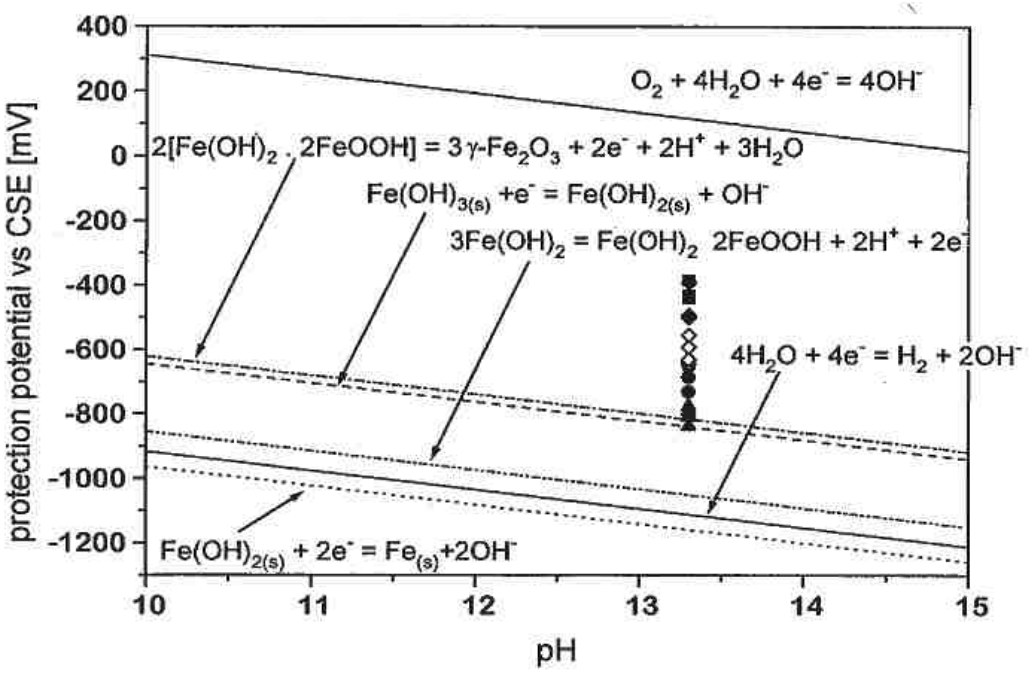

Fig. 12: Half-cell potentials of rebars during CP of specimens with varying chloride (0% ν, 1% υ, 3% σ) and a CP - Voltage of 1.6V (empty marks) and 2V (filled marks) in relation to the standard-half-cell-potentials of possible electrochemical reactions as function of pH.

Abb. 12: Halbzellenpotentiale von Bewehrungsstahl in Betonprismen mit unterschiedlichen Chloridgehalten (0% ν, 1% υ, 3% σ) *und einer Schutzspannung von 1.6V (leere Symbole) und 2V (gefüllte Symbole) im Vergleich zu den Halbzellenpotentialen möglicher elektrochemischer Reaktionen als Funktion des pH-Wertes.*

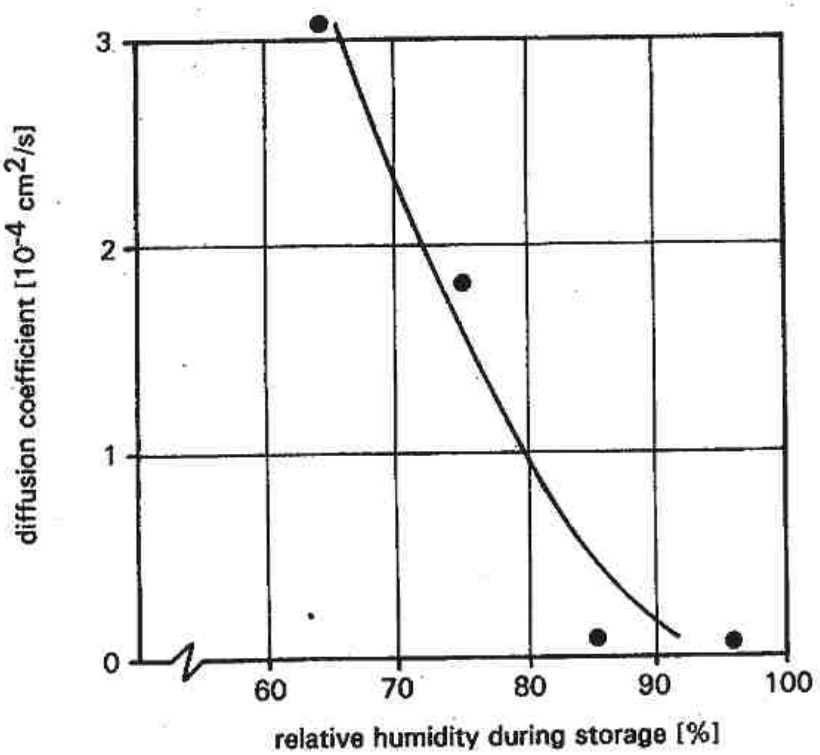

Fig. 13: Dependence of the diffusion coefficient for oxygen D_{O2} in concrete on the humidity during storage [45].

Abb. 13: Abhängigkeit des Diffusionskoeffizienten von Sauerstoff D_{O2} in Beton von der relativen Feuchte während der Lagerung [45].

Sufficient oxygen must be present near the rebar surface, in order for the reduction of oxygen to be the principal electrochemical reaction sustaining the cathodic protection current. The diffusion coefficient of oxygen in unsaturated concrete depends on the degree of saturation and therefore on the relative humidity at which the concrete specimens are stored (figure 13) [45].

The mass flow of oxygen for different distances between the surface of the concrete and the rebar can be calculated for static conditions using equation (2).

$$\Delta m = D.(c_1 - c_2).\frac{A}{L_{ep}} \qquad (2)$$

Δm ..... mass flow [g/m^{2}s]
D ..... diffusion coefficient [m^2/s]
Δt ..... time interval [s]
$c_1 - c_2$ ..... concentration gradient between the surface and the rebar [g/m^3]
A ..... surface area of the rebar [m^2]
L_{ep} ..... distance between the surface and the rebar [m] (figure 14)

For an estimated gas-diffusion coefficient $D_{O2} = 1 \cdot 10^{-8}$ m²/s, a distance between the rebar and the concrete surface of 0.02 m, an oxygen surface concentration of 252 g/m³ and a concentration gradient of 50% (126 g/m³), one obtains for the oxygen flow towards the rebar surface a value of $6.4 \cdot 10^{-5}$ g/m²s. This oxygen flow may sustain a cathodic reduction current of 760 mA/m², according to Faraday's law (equation 3).

$$Q = \frac{n \cdot F \cdot m}{M} \qquad (3)$$

Q .....electric charge [As]
n .....number of electrons per formula unit
F.....Faraday constant 96494 [As/mol]
m .....mass [g]
M.....molecular weight [g]

The maximum cathodic protection currents measured were below 50 mA/m², the largest average CP-currents were below 35 mA/m². Therefore, under the assumption that the open pore space extends to the rebar-surface and that the rebar surface is covered with only a thin layer of water, one may safely assume, that the CP-current is not controlled by the oxygen diffusion rate. At a current density of 35 mA/m², for an oxygen diffusion coefficient $D_{O2} = 1.9 \cdot 10^{-9}$ m²/s in solution [47] and a oxygen concentration of 0.21 Mol/m³ (7 ppm), the thickness of the diffusion layer in water is according to equation (4) [46] 2.4 mm, far larger than the thickness of the transition zone (L_{tz}) usually assumed (5 - 15 µm [30]) for the rebar/concrete interface.

(2) + (3)
$$i_{L_{O_2}} = \frac{-n F D_{O_2} c_{O_2}}{L_D} \qquad (4)$$

i_L.....limiting diffusion current [A/m²]
c_{O2}.....concentration of oxygen in the bulk solution [Mol/m³]
L_D .....thickness of the diffusion layer [m]

However, the diffusion of dissolved oxygen in the pore-water in concrete is restricted (due to the longer pathways) in comparison to the free solution by about one order of magnitude. Assuming a diffusion coefficient $D_{O2} = 2.1 \cdot 10^{-10}$ m²/s in water saturated concrete [48] one obtains according to equation (4) [46] for the maximum thickness L_{pw} of the water saturated concrete-pore-layer in front of the rebar surface (Figure 14) a value of ≈ 0.5 mm at a current density of 35 mA/m². This indicates that at $L_{pw} = 0.5$ mm, the limiting diffusion current is 35 mA/m² which corresponds to the maximum cathodic protection current at $L_{pw} > 0.5$ mm. The diffusion of oxygen through concrete up to storage humidities of 100% r.h. may be described as gas diffusion. From this, one may assume that the rebar surface is not surrounded entirely with water-filled pores at storage at 80% r.h.

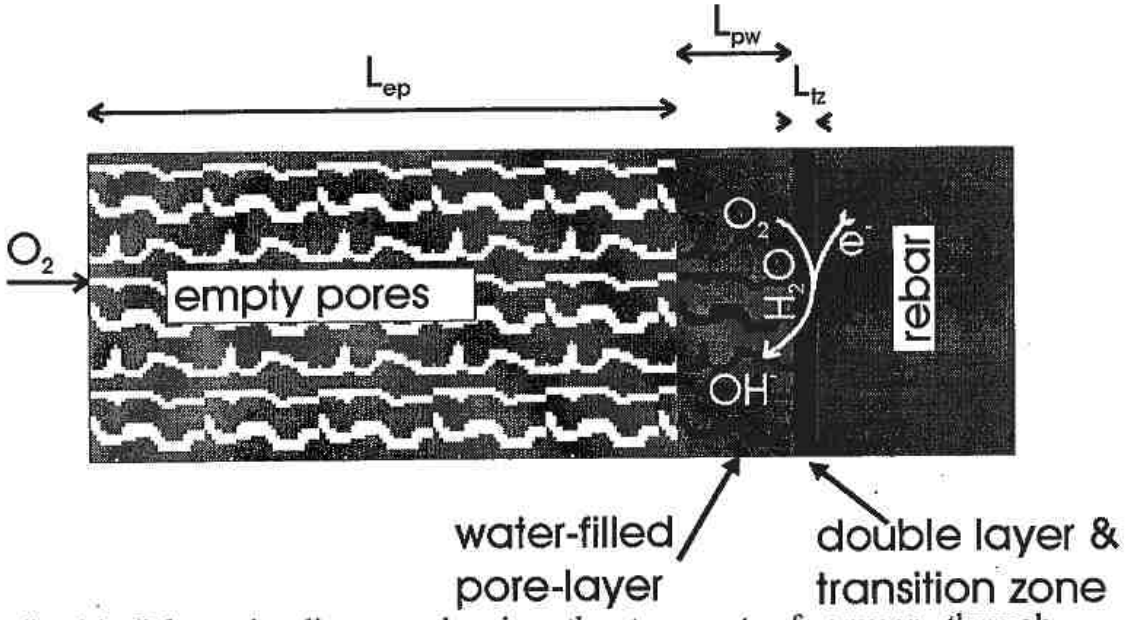

Fig. 14: Schematic diagram showing the transport of oxygen through concrete towards the rebar surface.

Abb. 14 Schematische Darstellung des Sauerstofftransportes von der Betonoberfläche an die Oberfläche des Bewehrungsstahles.

If the reduction of oxygen is the current sustaining electrochemical reaction (equation 1) during CP, then the OH^--ions produced will increase significantly the pH near the rebar surface. The OH^--ions produced will diffuse from the rebar surface into the surrounding concrete. As the transition zone between the rebar and the concrete is of the order of 5 to 15 µm in thickness [30] and the pore-space layer filled with water is smaller then 0.5 mm, one may assume, that the diffusion of OH^--ions from the rebar surface into the concrete matrix is mainly controlled by the diffusive properties of OH^--ions in the bulk concrete.

The diffusion of products of electrochemical reactions from the electrode surface into the electrolyte may be described by the SAND - equation [49] (equation (5)).

$$c_i = c_{i0} + \frac{I \cdot \nu_i}{n \cdot F} \cdot \frac{1}{\sqrt{\pi \, D_i}} \cdot \int_0^t \frac{1}{\sqrt{t}} \cdot \exp\left(-\frac{x^2}{4 \cdot D_i \cdot t}\right) dt \qquad (5)$$

c_i.....concentration of species i at the distance x in the bulk solution [mol/m3]

c_{i0}.....concentration of species i at the electrode surface [mol/m3]

I.....current [A/m^2]

ν.....reaction number

x.....distance from the electrode surface [m]

The diffusion of ions in the concrete matrix is usually investigated in concrete specimens saturated with water [50]. Diffusion coefficients are usually determined either on the basis of the Nernst-Planck equation (equation (6)) by electrical resistivity measurements or by the measurement of concentration gradients of ions

across a concrete plate immersed in two solutions with different ion concentrations [50]. The diffusion coefficient of chloride ions depends on the chloride ion concentration in the pore water due to the chloride binding activity of the cement matrix [51], at 3% total chloride content a value of $2 \cdot 10^{-12}$ m²/s is reported [52]. Diffusion coefficients $D_{Cl^-} = 2 - 50 \cdot 10^{-12}$ m²/s determined from chloride concentration profiles in real structures are reported [53]. To the best of our knowledge no values have been reported for the diffusion coefficients of OH^- in concrete. For the simulation of the OH^- - concentration profiles according to the SAND-equation (5) in the chloride-free and in 3% chloride containing specimens after switching-off CP, the diffusion coefficients D_{OH^-} were calculated from resistivity measurements according to equation (6). It is assumed that equation (6) is also valid in non-saturated concrete matrices.

$$D_i = \frac{R \cdot T}{n^2 \cdot F^2} \cdot \lambda_i = \frac{R \cdot T}{n^2 \cdot F^2} \cdot \frac{t_i}{\gamma_i \cdot c_i \cdot \rho} \qquad (6)$$

λ_i ..... conductivity at infinite dilution [$Ohm^{-1} mol^{-1} cm^2$]

t_i ..... $t_i = \frac{\lambda_i}{\sum_j \lambda_j}$

γ_i ..... activity coefficient

c_i ..... concentration in the pore-water [Mol/L]

ρ ..... resistivity [ohm.cm]

The diffusion coefficients listed in table 1 were calculated using the following values: $\lambda_{OH^-} = 199$, $\lambda_{K^+} = 73.5$, $\lambda_{Cl^-} = 76.4$ [$Ohm^{-1}mol^{-1}cm^2$] [54], $\gamma_{OH^-} = 0.7$ (0.2 - 1 mol KOH) [55]. The OH^- concentration in the concrete specimens before CP was taken as 0.2 mol/L (pH 13.3) in agreement with Page [18] and it was further assumed that the alkalinity is due to KOH only. The contribution of electromigration was estimated to be small (≤ 15%) due to the low potential drop between anode and cathode (25 mV < ΔE > 75 mV) and was not considered.

Table 1: Diffusion coefficients D_{OH^-} in concrete (w/c 0.50) stored at 80% humidity calculated from resistivity measurements, assuming a KOH concentration of 0.2 Mol/L in the pore-water.

chloride content		resistivity	D_{OH^-}
total chloride [%/wt. cement]	pore-water [Mol/L]	[kohm cm]	[m²/s]
0	0	49.1	2.8×10^{-12}
3	1.0	25.9	1.6×10^{-12}

Based on the calculated diffusion coefficients for OH^- (table 1) the spatial distribution of OH^- from the rebar surface into the concrete matrix was calculated for specimens with 0% and 3% chloride according to the SAND-equation (equation. (5)) after switching-off CP (figure 15). The average currents i were calculated from the charge consumed during CP (both are listed in figure 15). The OH^- -concentration- and the pH - profiles were calculated for a distance up to 15 mm from the rebar surface and on the assumption of a non-saturated concrete with a total porosity of 12.5 Vol.% (capillary porosity 11%) and a saturation at 80% r.h. of 50 Vol.%, determined from water-absorption measurements of the specimens before CP. The corresponding amount of acid, either as carbonic acid or hydrochloric acid (equations ((7) - (9)) is produced at the anode. Contribution from reaction (9) is expected only at the carbon filled polymer anodes.

$$2H_2O = O_2 + 2H^+ + 2e^- \quad (7)$$

$$2Cl^- = Cl_2 + 2e^- \quad (8a)$$

$$Cl_2 + H_2O = ClO^- + Cl^- + 2H^+ \quad (8b)$$

$$C + 2H_2O = CO_2 + 4H^+ + 4e^- \quad (9)$$

The acid (protons) produced at the anode will be neutralised initially by the portlandite ($Ca(OH)_2$) present in the concrete matrix and after the consumption of the portlandite by the cement gel. The acid neutralising capacity of concrete is according to Neville 19 Mol/m^2 mm [56]. From this the maximum acid neutralisation depth during the time period of CP is estimated to be less than 0.3 mm. With a concentration gradient of about 0.2 Moles OH^- across the neutralised layer, one may safely assume that the OH^- concentration resulting from the cathodic reaction will not be influenced by the acid produced at the anode at distances more than 5 mm from the anode surface.

Figure 15 shows that the pH at the rebar surface rises in all specimens to values of pH > 14. At the rebar surface of the specimens with a chloride content of 3% and with a Ti-mesh-anode showing the highest current consumption ($38.1 \cdot 10^4$ Cb/m^2), the pH rises above pH 15. The high pH near the rebar surface should influence significantly the rate of corrosion and the rest potentials of the rebars after switching-off CP.

The corrosion rate of steel in alkaline solutions depends on the ratio of Cl^-/OH^- according to Hausmann [25] who measured the corrosion rates of steelbars in alkaline solutions. These results [25] were corroborated by corrosion rate measurements of rebars immersed in artificial pore-solutions made from saturated portlandite solutions with various chloride contents [26]. The threshold between active and negligible corrosion (1 - 2 mA/m^2) or the depassivation threshold was found to be between Cl^-/OH^- ratios of 0.3 and 1 with a mean of 0.6 [26]. Page et al. [27] measured the dependence of the corrosion rate (i_{corr}) on the Cl^-/OH^- ratio in concrete specimens. The OH^- and Cl^- pore-solution concentrations were determined after the method of Longuet et al. [57] by exuding concrete specimens under a pressure of 350 MPA [18]. Page et al. [27] found a far higher critical value for the Cl^-/OH^- ratio of approximately 3 (figure 16).

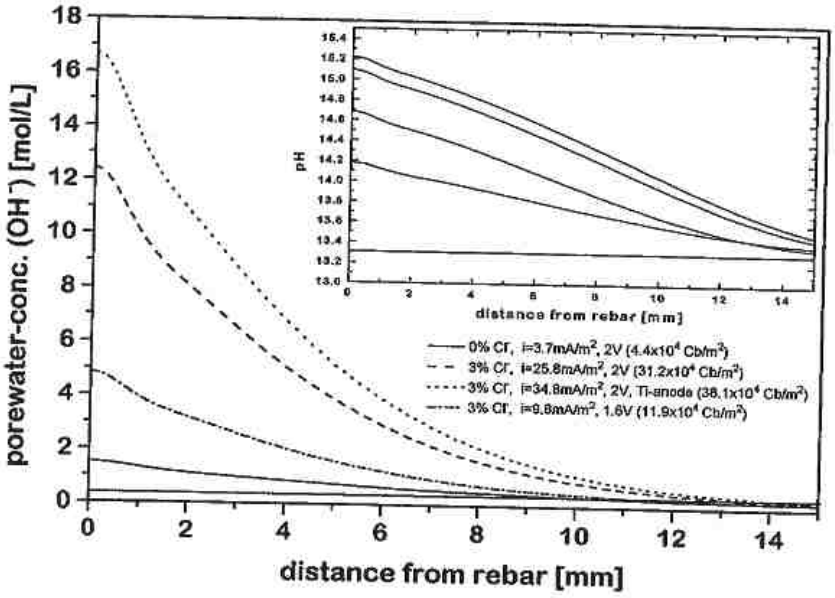

Fig. 15: OH^- - concentration and pH vs. distance from rebar according to Sand-equation after switching-off CP in concrete prisms with 3% chloride content and in the chloride-free reference prism.

Abb. 15: OH^- - Konzentration und. pH vs. dem Abstand von der Stahloberfläche, simuliert nach der Sand-Gleichung (Gl. 5), in Betonprismen mit einem Chloridgehalt von 3% und 0% nach dem Abschalten des Schutzstromes.

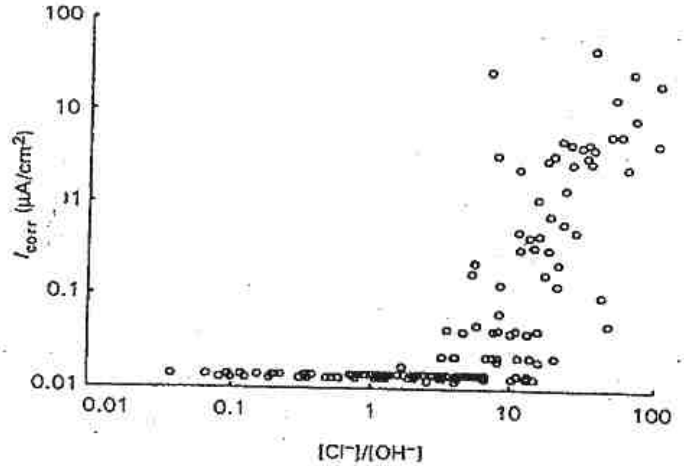

Fig. 16: Relation between corrosion rates and ratios of chloride/hydroxyl ion concentrations in pore solution of specimens exposed to chloride ingress [27]

Abb. 16: Abhängigkeit der Korrosionsraten von dem Chlorid/Hydroxylionen Konzentrationsverhältnis in der Porenlösung von Betonproben, die Trocken/Nass Tausalzzyklen ausgesetzt worden sind [27].

In order to examine the influence of the change of the Cl^-/OH^--ratio induced by the CP on the corrosion rates, the chloride concentrations in the pore solution were calculated from the potentials of a Ag/AgCl electrode embedded in the concrete specimens (figure 4). The Cl^-/OH^- ratios were calculated using the above values and the values for the OH^- - concentration obtained by the simulation using the Sand-equation. These were then plotted against the corrosion currents i_{corr} measured about two to three days after switching-off CP. The results are shown in figure 19. The linear regression line is calculated from corrosion rates before and after the application of CP. The corrosion rates of the rebars in concrete specimens before the application of CP correlate with the findings of Page et al. [27] insofar as a large scatter of corrosion rates at Cl^-/OH^--ratios > 3 is observed. However, the threshold value for active and insignificant corrosion (1 - 2 mA/m^2) is crossed at Cl^-/OH^- ratios close to the values reported by Goni et Andrade [26] and Hausmann [25] (Cl^-/OH^- 0.3 to 1.0 with a mean of 0.6).

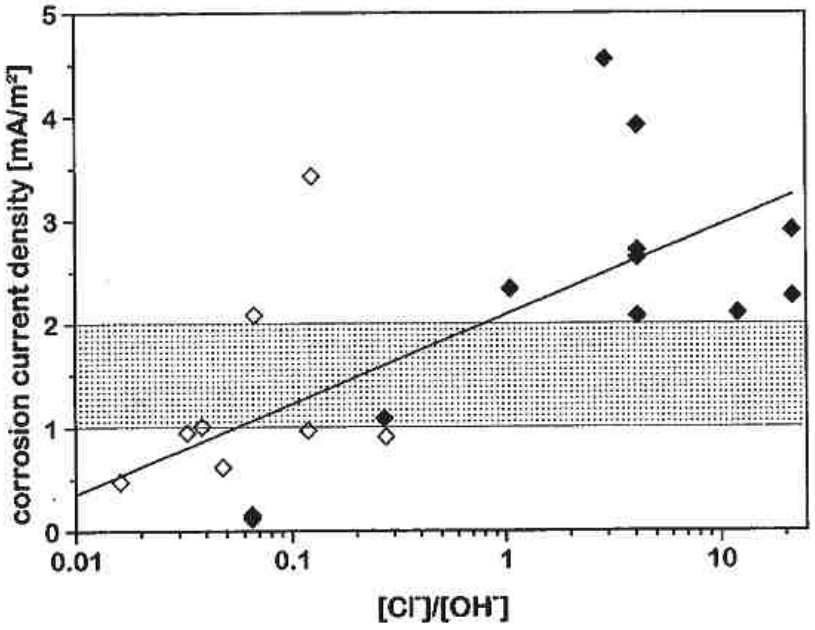

Fig. 17: Relation between corrosion rates and the ratios of Cl^-/OH^- - ion concentrations in pore solutions of specimens with varying chloride contents (1 - 3% weight cement) before (υ) and after (◊) CP.

Abb. 17: Abhängigkeit der Korrosionsraten vom Chlorid/Hydroxylionen Konzentrationsverhältnis in der Porenlösung von Betonprismen mit unterschiedlichen Chloridgehalten (1-3% des Zementgewichts) vor (υ) und nach (◊)Anlegen eines kathodischen Schutzstromes.

The critical value of the Cl^-/OH^--ratio of rebars after the application of CP appears to be significantly lower, close to a Cl^-/OH^-- ratio of 0.2, below the lower limit of the threshold value (0.3) [25,26]. Despite the scatter of the data the correlation between the Cl^-/OH^- ratio and the measured corrosion rates ($\log(i_{corr})$) is according to the F-Test statistics significant, for both, the values measured before ($F = 13.96$, $F_{crit.} = 0.007$) and after CP ($F = 48.6$, $F_{crit.} = 0.0009$). The in comparison with the Cl^-/OH^- threshold for the specimen before CP lower Cl^-/OH^- threshold value for the specimens after CP may be due to either higher Cl^- pore solution concentrations or lower OH^- - concentrations near the rebar surface then estimated. As electromigration effects on the OH- ions were not considered which might be not negligible especially near the rebar surface, the OH- concentration might therefore be lower then calculated by a factor of about three. The actual pH values might then be lower by 0.5 pH units (figure 15).

This indicates that the decrease of Cl^-/OH^- ratio due to the alkalisation and the high OH^- concentration accumulated at the rebar surface during CP (figure 15) has a significant influence on the repassivation of rebars after CP. The extent of the repassivation should then depend on the Cl^-/OH^- ratio near the rebar surface and the stability of the repassivation should depend on the diffusion of the OH^- due to the high concentration gradient from the rebar surface into the concrete matrix. The stability of the Cl^-/OH^- ratio near the rebar surface might be assumed to be proportional to the spatial extension of the "passivating" Cl^-/OH^- ratio from the rebar surface into the concrete matrix. As shown in figure 18, the specimens with high current consumption and therefore low Cl^-/OH^- ratios over several mm from the rebar surface are found to be stable over at least 40 days, whereas at higher more rapidly over the spatial distance changing Cl^-/OH^- ratios the repassivation decreases towards active corrosion within about 20 days (figure 10).

The rebar rest potentials decrease with increasing pH. In figure 19 the pH dependence of the rebar potentials of a rebar, taken out of one of the concrete prisms after about 6 months of curing and immersed in a saturated $Ca(OH)_2$-solution at pH values varying between 12.5 and 13.6 by the addition of KOH is shown.

By assuming a pH increase between 0.7 and 1.7 units during CP, the rebar potential after CP should move about 90 to 210 mV towards negative values. These values have to be added to the values E_{corr}-shift measured after CP (figure 9). This also implies that the corrosion potentials of the specimens with current consumptions $> 10^5$ Cb/m^2 are in the range of insignificant corrosion even after 110 days after CP (figure 7).

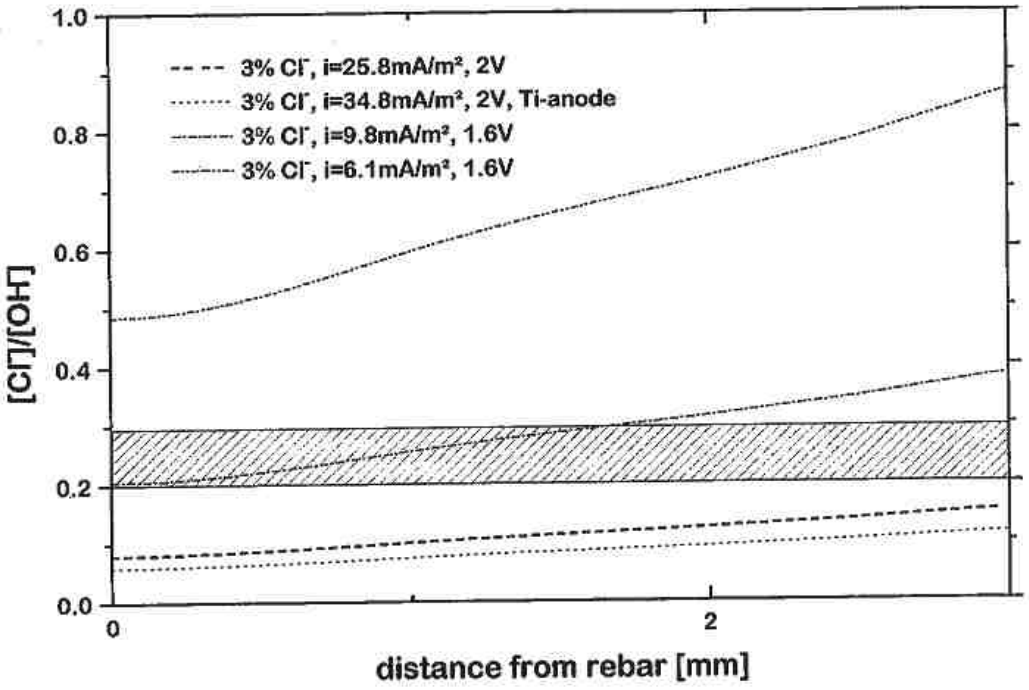

Fig. 18: Calculated Cl^-/OH^- ratios in concrete specimens (3% chloride) after CP as a function of the distance from the rebar surface.

Abb. 18: Berechnete Cl^-/OH^- Verhältnisse in Betonproben (3% Chlorid) nach Abschalten des Schutzstromes in Abhängigkeit der Entfernung von der Stahloberfläche.

The simulation of the OH- concentration profile after CP by the Sand-equation (5) is based on the assumption of a non-saturated concrete. Saturation of the concrete pore-system with water under static conditions should not change the Cl^-/OH^- ratio but would increase the apparent diffusion coefficient for OH^- and Cl^-. Saturation of the concrete matrix by immersion of the specimens into water, however, should modify the Cl^-/OH^- ratios as well as the absolute concentrations of OH^- and Cl^- near the rebar surface due to the influx of water by capillary suction into the concrete matrix. Water moving into the concrete matrix will then transport chloride ions dissolved in the matrix-pore-water across the rebar surface. The OH^- concentration, accumulated near the rebar surface should therefore be reduced through transport of fresh pore-water towards and across the rebar surface whereas the chloride-ion concentration should be less affected, thereby shifting the Cl^-/OH^- ratio towards higher values. Hence, immersion of specimens into water should increase the corrosion rates and consequently shift the corrosion potentials towards more positive values. This effect should be even more pronounced by immersion of the specimens into a salt solution.

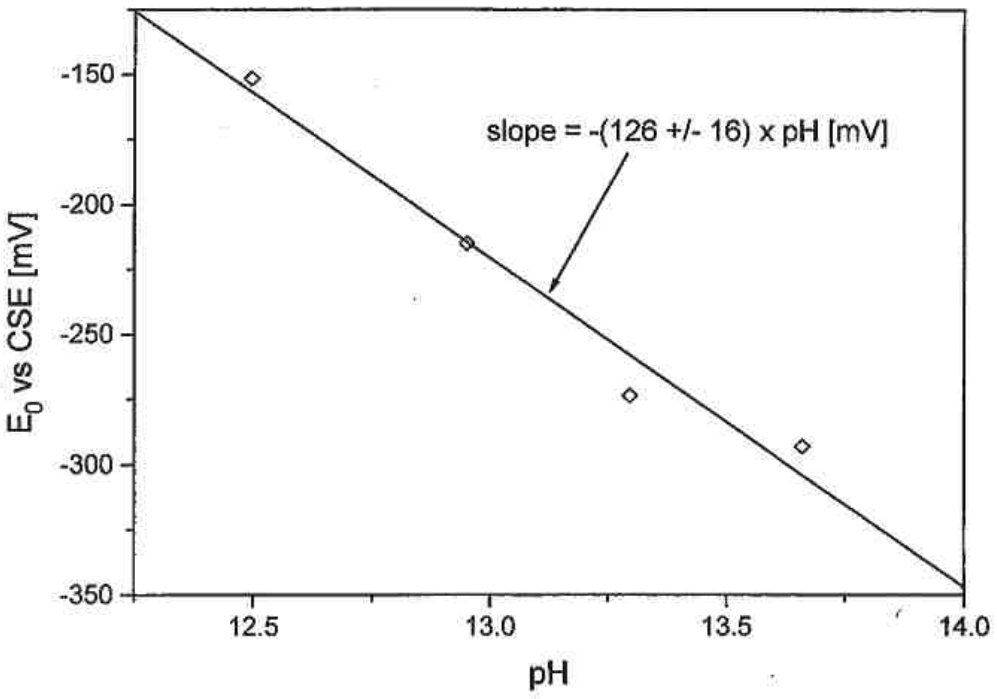

Fig. 19: Restpotential (corrosion potential) E_0 of a rebar immersed in a artificial pore-solution as a function of the pH.

Abb. 19: Ruhepotential (Korrosionspotential) E_0 eines Bewehrungsstahls in Abhängigkeit des pH-Wertes einer simulierten Porenlösung.

To evaluate the influence of the saturation of the concrete matrix by immersion in water or in salt solutions, specimens were stored for 24 h under water or exposed to three wet (3% NaCl-solution)/dry cycles.

After equilibration at 80% r.h. at ambient temperature, the corrosion currents and the corrosion potentials were determined by Tafel-measurements and by potential measurements vs. CSE. The equilibration proved to be especially important for the comparison of the corrosion currents i_{corr} before and after the immersion of the specimens in water and in 3% NaCl-solution whereas the corrosion potentials proved to be rather independent of the degree of saturation of the specimens. This is in agreement with the findings of Gonzalez et al. [43] which showed that the corrosion currents of rebars in chloride containing concrete specimens are strongly dependent on the storage humidity and may increase by nearly two orders of magnitude by increasing the humidity from 40% r.h. to 100% r.h. over a time period of about 20 days whereas the corrosion currents of rebars in chloride-free samples are nearly independent of the storage humidity. To achieve nearly the same humidity conditions as before immersion, the specimens had to be dried first at 50° C for about 3 days and then stored at 80% r.h. and ambient room temperature for 2 days.

In figure 20, the effects of the immersion of concrete specimens with varying chloride contents (0% - 3% chloride) and varying anode materials into water are shown: (a) before CP, (b) approximately 110 days after switching-off CP and (c) 24 h storage under water and equilibration at 80% r.h. In none of the specimens is the potential E_{corr} before CP reached. The corrosion potentials E_{corr} are not significantly influenced by the immersion into water except for the specimen with 3% chloride (3) which shows a shift towards positive potentials (less corrosive) of about +60 mV and the chloride-free reference specimen which shows an potential shift of +30 mV. This indicates, that the water flow by capillary suction through the concrete matrix during immersion into water and successively during drying and equilibration does not induce higher corrosion rates and thus has no significant influence on the repassivation induced by CP. For the specimen with the highest spatial OH^- concentration gradient (4), a shift of E_{corr} towards a more corrosive state before CP would have been expected but an opposite shift towards less corrosion is observed.

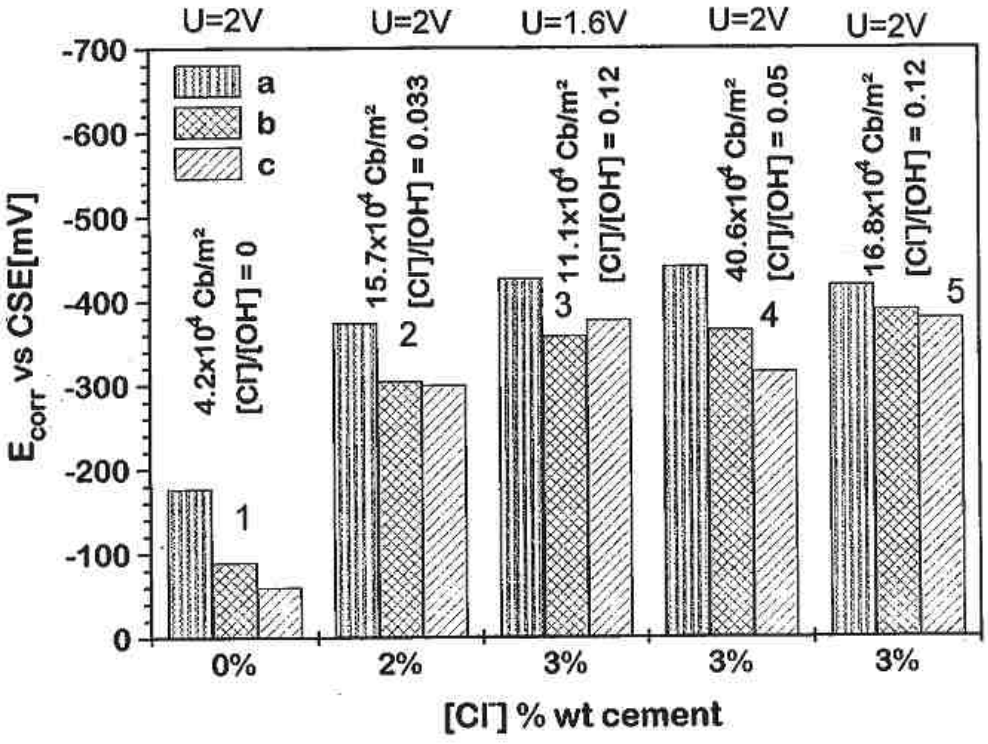

Fig. 20: Corrosion potentials E_{corr} before CP, about 110 days after CP and after 24 h storage under water, drying at 50° C and equilibration at 80% r.h..

Abb. 20: Korrosionspotentiale E_{corr} vor, ca 110 Tage nach dem Ausschalten des Schutzstromes und nach 24-stündiger Wasserlagerung, Trocknen bei 50° C und Equilibrierung bei 80% r.F.

In figure 21 and figure 22 the effect of repeated immersion into a 3% NaCl-solution after drying at 50°C on the corrosion potential E_{corr} and the corrosion currents I_{corr} is shown. As expected, the most pronounced effect is observed in the chloride-free specimen (1). After three wet/dry cycles, E_{corr} shifts by about -340 mV from a state of insignificant corrosion towards a state of active corrosion (figure 21). However, the corrosion current I_{corr} increases only from about 0.12 mA/m^2 to 0.45 mA/m^2 (figure 22), significantly below the threshold for active corrosion [18,26]. The state of corrosion of the rebars in the chloride containing specimens is changed significantly during the wet/dry cycles only in the specimen 2 and specimen 6. The change of the corrosion potential E_{corr} does not always correlate with the change of I_{corr} and vice versa.

As can be seen from figures 21 and 22, there are significant shifts of E_{corr} for specimen 1 & 2 towards a more corrosive state (not accompanied by corresponding increases of I_{corr}) while for specimen 4 significant changes in I_{corr} are not accompanied by corresponding changes of E_{corr}. As E_{corr} is less dependent on the humidity of the samples than I_{corr} the former ones are more reliable than i_{corr} in showing the effects of the wet/dry cycles upon the state of corrosion.

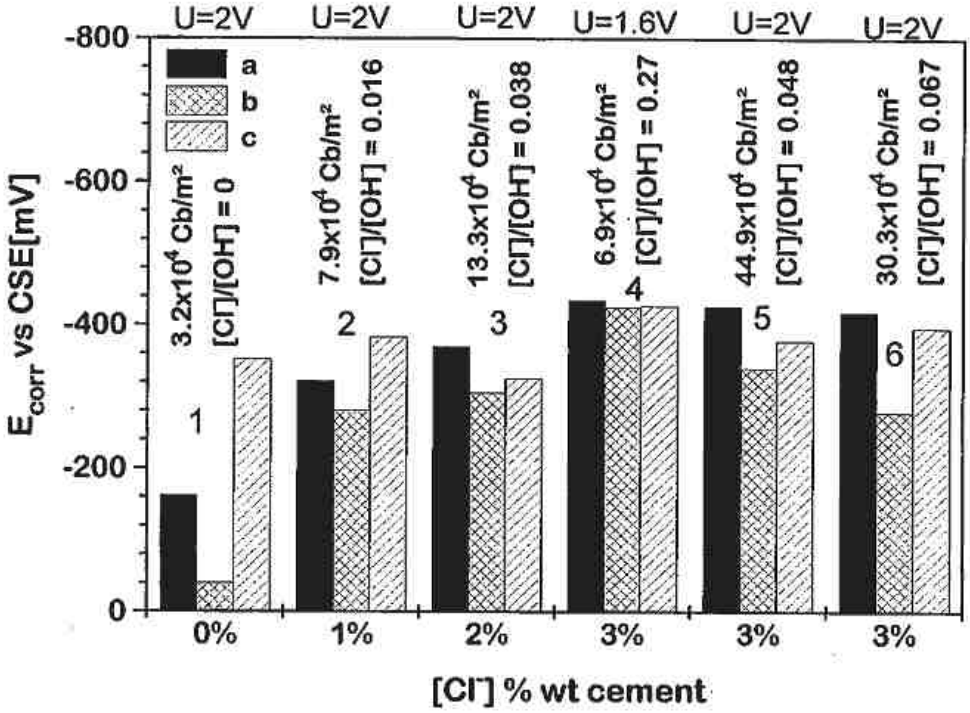

Fig. 21: Corrosion potentials E_{corr} before CP, about 110 days after CP and after three wet/dry cycles under 3% NaCl - solution, drying at 50° C and equilibration at 80% r.h..

Abb. 21: Korrosionspotentiale E_{corr} vor, ca 110 Tage nach dem Ausschalten des Schutzstromes und nach drei Trocken/Nass-Zyklen mit 3%iger NaCl-Lösung, Trocknen bei 50° C und Equilibrierung bei 80% r.F.

Relying on E_{corr} (figure 21) as a measure for the effect of wet (3% NaCl-solution)/dry cycles on the state of corrosion, then the following tendencies are found:

Repeated immersion into 3% NaCl-solution with subsequent drying increases the corrosivity except for specimens, in which the repassivation of the rebar has nearly vanished already before the wet/dry cycles (e.g., specimen 4). In the specimens 1 and 2, with the lowest charge consumed during CP, the state of corrosion is shifted to a more corrosive state than before the wet/dry cycles and even before CP. However, specimen 6 with a high current consumption during CP shows a strong shift towards negative potentials after the wet/dry cycles, but remains below E_{corr} before CP. In all cases, the most stable specimens with respect to E_{corr} and I_{corr} are those with the lowest Cl^-/OH^- ratio (< 0.1). The highest stability of repassivation is shown by the specimen with a Ti-mesh anode polarised with 2V. The results indicate that a minimum current consumption during CP, resulting in the formation of OH^-, is necessary to stabilise the repassivation with regard to chloride intrusion by wet/dry cycles.

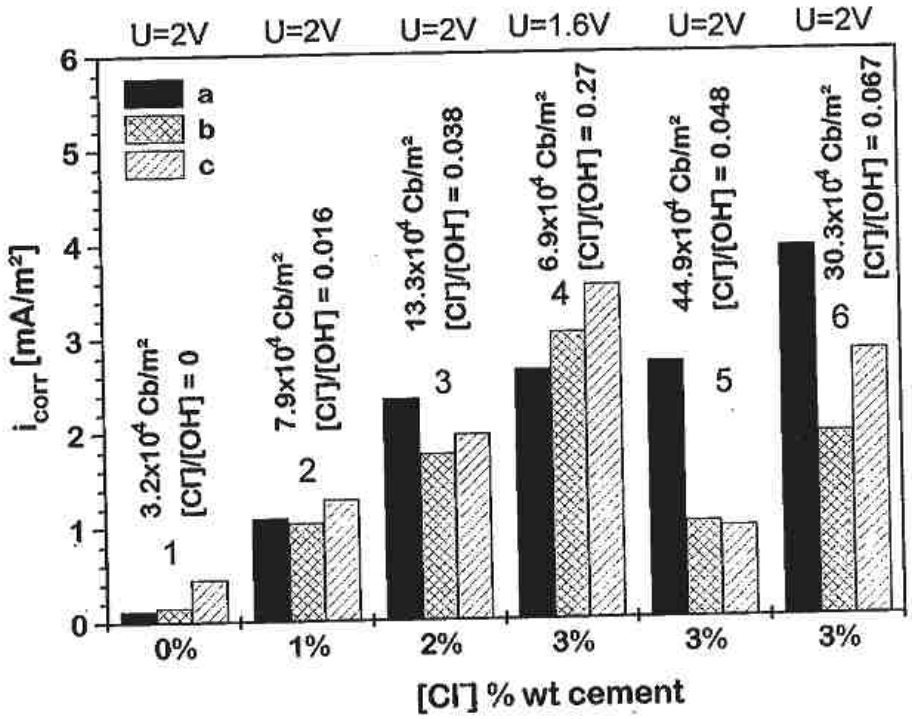

Fig. 22: Corrosion currents I_{corr} before CP, about 110 days after CP and after three wet/dry cycles under 3% NaCl - solution, drying at 50° C and equilibration at 80% r.h..

Abb. 22: Korrosionsströme I_{corr} vor CP, ca 110 Tage nach dem Ausschalten des Schutzstromes und nach drei Trocken/Nass-Zyklen mit 3%iger NaCl-Lösung, Trocknen bei 50° C und Equilibrierung bei 80% r.F.

The stability increases with decreasing Cl^-/OH^- ratios. The relatively low sensitivity of the corrosion potentials E_{corr} towards water saturation and drying of the concrete specimens and of E_{corr} and I_{corr} of chloride containing concrete specimens towards chloride intrusion by wet/dry cycles indicates, that the change of the Cl^-/OH^- ratio does not by itself explain the repassivation of rebars, especially the stability of the repassivation after CP.

During CP, the high field gradient in the passive layer ($\approx 10^5$ V/cm) and the OH^- ions produced (electroneutrality principle) induce the removal of chloride ions from the rebar surface and from the electric double layer. The chloride ions will move into the outer passive layer [15] or even beyond, supported by the electric field gradient (electromigration). The outer layer consists of green rust ($Fe_4(OH)_8Cl$), akaganeite β-(FeO(OH,Cl)) and δ-FeO(OH) at chloride ion concentrations between 0.01% and 1% and pH 12.5 [15]. These types of iron-hydroxo-chloro complexes formed, determine the mobility of the chloride ions between the outer and the inner layer [15]: In the absence of CP, Fe(II) is transported by the diffusion of iron-hydroxo-chloro complexes to the outer layer/concrete boundary, where they eventually precipitate as iron(III)hydroxides, owing to the higher oxygen concentration near the end of the diffusion layer. The liberated chloride ions are attracted back to the anodic corrosion sites on the rebar.

During CP, the chloride ions are repulsed by the negatively charged rebar and tend to move towards the exterior anode. The accumulation of OH^- near the rebar surface results in the destabilisation of the iron-hydroxo-chloro complexes. At Cl^-/OH^- ratios < 1.025, iron-hydroxo-chloro-complexes (e.g. green rust) are not stable [44]. During the repassivation process after CP, the oxygen diffusion layer tends to decrease with the consequence that the oxygen concentration increases near the rebar surface. $Fe(OH)_2$ formed as an intermediate is then directly oxidised to hydrated magnetite $Fe(OH)_2.2FeOOH$ (figure 12) [44] with the final formation of magnetite Fe_3O_4. Magnetite is the main constituent of black rust, which forms a protective layer on iron surfaces corroding under oxygen deficiency [58]. Therefore, one may assume that the outer layer adjacent to the inner passive layer is transformed into hydrated magnetite and consecutively to magnetite, which forms a protective layer around the rebar. Due to the high pH, the surface of the magnetite or that of the hydrated magnetite will be charged negatively [59]. This hinders the diffusion of Cl^- towards the inner passive layer. At pH 14 to pH 15, the solubility of Fe(II) as ferrite anion ($HFeO_2^-$) is of the order of 10^{-4} to 10^{-3} Mol/L [60], sufficiently high to react with $Ca(OH)_2$ to form nearly insoluble calcium-ferrites. The inclusion of co-precipitated $Ca(OH)_2$ into the passive layer of iron is known to enhance passivity [61]. Furthermore, in the high pH region (pH > 14) eventually the surface of silicious aggregates might be partially dissolved and the alkali-calcium-silica gel formed by a localised alkali-silica reaction may provide an additional physical barrier to the diffusion of chloride ions.

Hence, on the assumption that after the transfer of sufficient charge during CP and consequent accumulation of OH^- at the rebar surface to such an extent that the Cl^-/OH^- ratio falls significantly below 1, a protective layer is formed which probably

consists of hydrated magnetite, magnetite and eventually γ-Fe_2O_3 and γ-FeOOH (see figure 12), doped with Ca^{2+}-ions. On rebars in concrete specimens containing 3% chloride by weight of cement, on which CP was applied for about 4 years, a continious black layer is formed which in some areas is covered with easily removable brown products [62], in agreement with the model described above. The results suggest that the thickness of the secondary protective layer depends not only on the thickness of the outer passive layer but also on the amount of corrosion products present near the rebar surface before application of CP. The secondary protective layer will be stable as long as the Cl^-/OH^- - ratio remains significantly below 1. However, even after the Cl^-/OH^- ratio will have increased due to the diffusion of OH^-, the secondary protective layer will retard the depassivation of the primary passive layer for some time as observed (figure 20 - 22).

5 Conclusions

Prolonged application of CP to the reinforcement induces a shift of the corrosion potentials E_{corr} to more positive values after CP, in chloride containing specimens also a significant reduction of the corrosion currents I_{corr} is observed which is interpreted as at least partial repassivation caused by CP. The extent and the stability of the repassivation depend on the charge consumed during CP and on the Cl^-/OH^- - ratio at the rebar/concrete interface which is shifted towards smaller values due to OH^- produced at the rebar surface during CP. At lower chloride contents less charge has to be consumed during CP. The influence of the Cl^-/OH^- ratio on the corrosion rates reported by several authors [25-27] is interpreted to be due to the stabilisation/destabilisation of iron(II)hydroxo-chloro complexes which are formed during chloride induced pitting corrosion in the outer passive layer [15]. These complexes are not stable below a Cl^-/OH^- ratio of 1 [44]. At Cl^-/OH^- ratios significantly below 1 (< 0.2) a secondary protective layer is formed, consisting mainly of magnetite. This secondary protective layer adheres to the rebar surface and provides additional protection against chloride induced corrosion. Therefore CP may be also regarded as a soft realkalisation method providing additional corrosion protection due to the formed secondary protective layer without the potentially damaging effects of hydrogen generated during full-scale realkalisation.

6 Reference

1 RILEM Technical Comittee 124SRC, *Draft recommendation for repair strategies for concrete structures damaged by reinforcement corrosion*, Mater. Struct. **27**, 415 - 436 (1994)

2 B.S. Wyatt, *Cathodic protection of steel in concrete*, Corros. Sci. **35**, 1601 - 1615 (1993)

3 P. Pedeferri, G. Mussinelli and M. Tettamanti, *Experiences in anode materials and monitoring systems for cathodic protection of steel in concrete*, in "Corrosion of reinforcement in concrete" Page, C.L., Treadaway, K.W.J., Bamforth, P.B., editors, Elsevier, London, pp. 408 - 506 (1990)

4 F. Hunkeler, *Untersuchungen zum kathodischen Korrosionsschutz von Stahlbeton im Tunnel San Bernardino*, Vereinigung Schweizerischer Strassenfachleute, Zürich (1992).

5 T. Pastore, P. Pedeferri, L. Bertolini and F. Bolzoni, *Current distribution problems in the cathodic protection of RC structures*, in Proceedings RILEM Intern. Conf. on the Rehabilitation of Concrete Structures, Ho, D.W.S., Collins, F., editors, Melbourne, pp. 189 - 200 (1992)

6 L. Bertolini, F. Bolzoni, A. Cigada, T. Pastore and P. Pedeferri, *Cathodic protection of new and old reinforced concrete structures*, Corros. Sci. **35**, 1633 - 1639 (1993)

7 *Cathodic protection of reinforced concrete*, Technical Report No. 36, Concrete Society, London (1989)

8 R.O. Müller und K. Holtzhauer, *Kathodischer Korrosionsschutz von Bewehrungsstählen - Langzeitbeständigkeit: Anodenmaterialien und Mörtel,* Forschung im Strassenwesen des ASB/EVED, Forschungsauftrag Nr. 88/89, Schlussbericht (1992)

9 NACE, *Standard Recommended Practice: cathodic protection of reinforcing steel in atmospherically exposed concrete structures,* NACE Standard RP0290-90/53072 (1990)

10 G. Sergi, C.L. Page and D.M. Thompson, *Electrochemical induction of alkali-silica reaction in concrete*, Mater. Struct. **24**, 359 - 361 (1991)

11 K. Menzel, *Einige theoretische Aspekte des kathodischen Korrosionsschutzes von Stahl in Beton,* in Werkstoffe und Konstruktion I, FMPA Baden Württemberg, Editor, Stuttgart, pp. 179 - 190 (1989)

12 W.F. Perenchio, J.R. Landgren, R.E. West and K.C. Clear, *Cathodic protection of concrete bridge substructures*, National Cooperative Highway Research Program Report **278**, p.31 (1985)

13 W.K. Green, S.B. Lyon and J.D. Scantlebury, *Electrochemical changes in chloride contaminated reinforced concrete following cathodic polarisation,* Corros. Sci. **35**, 1627-1631 (1993)

14 W. Schwarz, F. Pruckner, J. Theiner, G.E. Nauer and J. Eri, *Evaluation of the efficiency of the cathodic protection of reinforced concrete by monitoring the electrical resistivity using linear polarisation techniques and electrochemical impedance spectroscopy (EIS)*, Internationale Zeitschrift für Bauinstandsetzen **2**, 33 - 48 (1996)

15 K.K. Sagoe-Crentsil and F.P. Glasser, *Analysis of the steel:concrete interface* in Corrosion of reinforcement in concrete, Page, C.L., Treadaway, K.W.J., Bamforth, P.B., editors, SCI, Elsevier, London, pp. 408 - 506 (1990)

16 Z.P. Bazant, *Physical model for steel corrosion in concrete sea structures-theory*, J. of the Structural Division ASCE **105**, 1137 - 1153 (1979)
17 C.L. Page and K.W.J. Treadway, *Aspects of electrochemistry of steel in concrete*, Nature **297**, 109 - 114 (1982)
18 C.L. Page, P. Lambert, *Investigations of reinforcement corrosion. 1. The pore electrolyte phase in chloride-contaminated concrete*, Mater. Struct. **24**, 243 - 252 (1991)
19 S. Mindess, *Interfaces in concrete,* in Materials Science of Concrete I, Ed. Skalny, J.P., American Ceramic Society, Westerville, pp 163 - 180 (1989)
20 A. Bentur, S. Diamond and S. Mindess, *The microstructure of the steel-fibre cement interface*, J. Mater. Sci. **20**, 3610 - 20 (1985)
21 C.L. Page, *Mechanism of corrosion protection in reinforced concrete marine structures,* Nature **258**, 514 - 515 (1975)
22 C.L. Page, *Microstructural features of interfaces in fibre cement*, Composites, 140 - 44 (1982)
23 P., Schiessl, M. Raupach, *Influence of concrete composition and microclimate on the critical chloride content in concrete*, in Corrosion of reinforcement in concrete, Page, C.L., Treadaway, K.W.J., Bamforth, P.B., editors, SCI, Elsevier, London, pp. 49 - 58 (1990)
24 ACI-Committee 201, *Guide to durable concrete*, J. Amer. Concr. Inst. **74**, 573 - 609 (1977), **75**, 269 - 73 (1978)
25 D.A. Hausmann, *Steel corrosion in concrete*, Mater. Protection **6**, 19 - 23 (1967)
26 S. Goni and C. Andrade, *Synthetic concrete pore solution chemistry and rebar corrosion rate in the presence of chlorides,* Cement Concr. Res. **20**, 525 - 539 (1990)
27 P. Lambert, C.L. Page and P.R.W. Vassie, *Investigations of reinforcement corrosion. 2. Electrochemical monitoring of steel in chloride-contaminated concrete*, Materials and Structures **24**, 351 - 358 (1991)
28 A.J. Arvia, *Active-passive transition in metals,* Proceedings of 8th Intern. Congr. Metallic Corr., 1981, Mainz, pp. 2065-80 (1981)
29 R.T. Foley, *Role of chloride ions in iron corrosion,* Corrosion-NACE **26**, 58-70 (1970)
30 D.S. Leek, A.B. Poole, *The breakdown of the passive film on high yield mild steel by chloride ions* in Corrosion of reinforcement in concrete, Page, C.L., Treadaway, K.W.J., Bamforth, P.B., editors, SCI, Elsevier, London, pp. 408 - 506. (1990)
31 N. Sato, *A theory for breakdown of anodic oxide films on metals,* Electrochim. Acta **16**, 1683 - 1692 (1971)
32 K.K. Sagore-Crentsil and F.P. Glasser, *Constitution of green rust and its significance to the corrosion of steel in Portland cement*", Corrosion **49**, 457 - 463 (1993)

33 C. Alonso, C. Andrade and J.A. Gonzalez, *Relation between resistivity and corrosion rate of reinforcement in carbonated mortar made with several cement types*, Cement Concr. Res. **18**, 687 - 698 (1988)

34 K. Suda, S. Misra and K. Motohashi, *Corrosion products of reinforcing bars embedded in concrete*, Corros. Sci **35**, 1543 - 1549 (1993)

35 H. Laase und W. Stichel, *Stützwandsanierung in Berlin: Spezielle Aspekte der Korrosion an der Rückwand*, Bautechnik **60**, 124 - 129 (1983)

36 P.K. Mehta, P. Schiessl and M. Raupach, *Performance and durability of concrete systems,* Proceedings of the 9th ICCC, New Delhi, India, **I**, p. 622. (1992)

37 SGK Richtlinie C7d, *Richtlinie für Projektierung, Ausführung und Überwachung des Kathodischen Korrosionsschutzes von Stahlbetonbauwerken,* Schweizerische Gesellschaft für Korrosionsschutz, Seefeldstr. 301, CH-8034 Zürich (1991)

38 J. Theiner, Inst. physikalische Chemie, Universität Wien, A-1090 Wien.

39 F. Pruckner, J. Theiner, J. Eri and G.E. Nauer, *In-situ monitoring of the efficiency of the cathodic protection of reinforced concrete by electrochemical impredance spectroscopy,* Electrochim. Acta **41**, 1233-1238 (1996)

40 C. Andrade and J.A. Gonzalez, *Prediction of potential corrosivity of concrete additives by the joint determination of pitting potential and polarisation resistance*, Research Working Papers, Instituto Eduardo Torroja, Madrid, Spain, No. 33, June (1978)

41 M. Molina, *Zerstörungsfreie Erfassung der gelösten Chloride im Beton*, Dissertation ETH Nr. 10315, ETH-Zürich (1993)

42 C. Andrade, C. Alonso and J.A. Gonzalez, *Results of polarization resistance and impedance of steel bars embedded in carbonated concrete contaminated with chlorides*, Materials Science Forum **44 & 45**, 329 - 336 (1989)

43 J.A. Gonzalez, A. Feliu, P. Rodriguez, E. Ramirez, C. Alonso and C. Andrade, *Some questions on the corrosion of steel in concrete-part 1: when, how and how much steel corrodes,* Mater. Struct. **29**, 40 - 46 (1996)

44 Ph. Refah and J.-M. Genin, *The oxidation of ferrous hydroxides in chloride-containing aqeous media and Pourbaix diagrams of green rust one*, Corros. Sci. **35**, 797 - 819 (1993)

45 H. Hurling, *Oxygen permeability of concrete*, in Proc. RILEM Seminar on Durability of Concrete Structures under Normal Outdoor Exposure, Hannover, pp. 91-101, March (1984)

46 J.A. Gonzalez, S. Feliu, P. Rodriguez, W. Lopez, E. Ramirez, C. Alonso and C. Andrade, *Some questions on the corrosion of steel in concrete-part 2: corrosion mechanism and monitoring, service life prediction and protection methods,* Mater. Struct. **29**, 97-104 (1996)

47 R.E. Davis, G.L. Horvath and C.W. Tobias, *The solubility and diffusion coefficient of oxygen in potassium hydroxide solution*, Electrochim. Acta **12**, 287 - 297 (1967)

48 O.E. Gjorv, O. Vennesland and A.H.S. El-Busaidy, *Diffusion of dissolved oxygen through concrete,* Materials Performance **25**, 39 - 44 (1986)

49 K.J. Vetter, *Elektrochemische Kinetik,* Springer, Berlin, pp 182(1961)
50 G. Mette, H. Grube, L. Tang, L.-O. Nilsson and C. Andrade, *Laboratory test methods*, in Performance Criteria for Concrete Durability, RILEM REPORT **12**, Kropp, J., Hilsdorf, H.K. editors, E&FN Spon, London, pp. 213 - 257 (1995)
51 L.-O. Nilsson, L. Tang, *Transport Mechanisms in Porous Materials,* in The Modelling of the Microstructure and its Potential for Studying Transport Properties and Durability, Jennings, H., Kropp, J., Scrivener, K., editors, NATO ASI-Series E: Applied Science Vol **304**, Kluwer, Dordrecht, pp. 289 - 312. (1996)
52 L.-O. Nilsson, M. Massat and L. Tang, *The effect of non-linear chloride binding on the prediction of chloride penetration into concrete structures*, Proc. 3rd CANMET/ACI Intl. Conf. on Durability of Concrete, ACI SP-145, 469-486 (1994)
53 P.S. Mangat and B.T. Molloy, *Prediction of long term chloride concentration in concrete*, Mater. Struct. **27**, 338 - 346 (1994)
54 Ch.M.A. Brett and A.M.O. Brett, *Electrochemistry Principles, Methods and Applications*, Oxford University Press, Oxford, p. 31 (1993)
55 C. Andrade, M. Castellote, D. Cervignon and C. Alonso, *Chloride migration in concrete: theory and modelling*, Intern. Zeitschr. Bauinstandsetzen **1**, 485 - 507 (1995)
56 A.M. Neville, *Properties of concrete*, Longman Scientific, Harlow Essex, U.K. p. 456 (1993)
57 P. Longuet, L. Burglen et A. Zelwer, *La phase liquide du ciment hydraté,* Rev. Mater. Constr. Trav. Publics, 35 - 41 (1973).
58 Tuutti, Kyösti, *Corrosion of steel in concrete*, CBI, Stockholm, p. 297. (1982)
59 W. Stumm, *Chemistry of the solid-water interface,* Wiley, New York, p. 69 (1992)
60 Ch.F. Baes and R.E. Mesmer, *The hydrolysis of cations*, Krieger, Malabar, Fl p 236 (1986)
61 O.A. Albani, L.M. Gassa, J.O. Zerbino, J.R. Bilche and A.J. Arvia, *Comparative study of the passivity and the breakdown of passivity of polycrystalline iron in different alkaline solutions,* Electrochim. Acta **35**, 1437 - 1444 (1990)